Pricing Catastrophic Bonds for Earthquakes in Mexico

Master Thesis submitted to

Prof. Dr. Wolfgang Härdle

Institute for Statistics and Econometrics

CASE - Center for Applied Statistics and Economics

Master in Economics and Management Science

Humboldt-Universität zu Berlin

by

Brenda López Cabrera

(500113)

in partial fulfillment of the requirements

for the degree of

Master of Sciences in Economics and Management Science

Berlin, October 4, 2006

Supported by the Programme Alβan, the European Union Programme of High Level Scholarships for Latin America, scholarship No.E04M049436MX.

Declaration of Authorship

I hereby confirm that I have authored this master thesis indepently and without use of others than the indicated sources. All passages which are literally or in general matter taken out of publications or other sources are marked as such.

Berlin, October 4, 2006.

Brenda López Cabrera

Abstract

After the occurrence of a natural disaster, the reconstruction can be financed with catastrophic bonds (CAT bonds) or reinsurance. For insurers, reinsurers and other corporations CAT bonds provide multi year protection without the credit risk present in reinsurance. For investors CAT bonds offer attractive returns and reduction of portfolio risk, since CAT bonds defaults are uncorrelated with defaults of other securities. As the study of natural catastrophe models plays an important role in the prevention and mitigation of disasters, the main motivation of this thesis is the pricing of CAT bonds for earthquakes in Mexico. This thesis examines the calibration of a real parametric CAT bond for earthquakes that was sponsored by the Mexican government. This thesis also derives the price of a hypothetical modeled loss CAT bond for earthquakes, which is based on the compound doubly stochastic Poisson pricing methodology from Baryshnikov et al. (1998) and Burnecki and Kukla (2003).

Keywords: Earthquakes, CAT bonds, Reinsurance, Trigger mechanism, Compound doubly Poisson process

Contents

List of Figures

List of Tables

Notation of abbreviations

cdf	Cumulative distribution function
d	Depth of an earthquake
e.g.	Exempli gratia; for example
edf	Empirical distribution function
et al.	among others
i.e.	id est.; that is
Mw	Magnitude Richter Scale of an earthquake
T	Expiration time
τ	Threshold time event
λ_t	Intensity rate
$(\Omega, \mathcal{F}, \mathcal{F}_t, P)$	Probability space
$\phi(x)$	The standard normal
$\hat{l}_n(x)$	Empirical limited expected function
$l(x)$	Analytical limited expected value function
$\hat{e}_n(x)$	Empirical mean excess function
$e(x)$	Mean excess function
$\mathrm{E}(x)$	Expected value function
X_k	Adjusted losses
$I_{(0,1)}$	Indicator of impact on Mexico City
N_t	Flow process of a natural event
CAT	Catastrophic
CB	Coupon CAT bond
HPP	Homogeneous Poisson Process
ILS	Insurance Linked Securities
LIBOR	London Inter-Bank Offered Rate
MAD	Mean of the absolute differences
MAVRD	Mean of the absolute values of the relative differences
NHPP	No Homogeneous Poisson Process
SPV	Special Purpose Vehicle
ZCB	Zero Coupon CAT bond

1 Introduction

By its geographical position, Mexico finds itself under a great variety of natural phenomena which can cause disasters, like earthquakes, eruptions, hurricanes, burning forest, floods and aridity (dryness). In case of disaster, the effects on financial and natural resources are huge and volatile.

In Mexico the first risk to transfer is the seismic risk, because although it is the less recurrent, it has the biggest impact on the population and country. For example, an earthquake of magnitude 8.1 Mw Richter scale that hit Mexico in 1985, destroyed hundreds of buildings and caused thousand of deaths. The Mexican insurance industry officials estimated payouts of four billion dollars.

After the occurrence of a natural disaster, the reconstruction can be financed with catastrophic bonds (CAT bonds) or reinsurance. For insurers, reinsurers and other corporations CAT bonds provide multi year protection without the credit risk present in reinsurance. For investors CAT bonds offer attractive returns and reduction of portfolio risk, since CAT bonds defaults are uncorrelated with defaults of other securities. As the study of natural catastrophe models plays an important role in the prevention and mitigation of disasters, the main motivation of this thesis is the pricing of CAT bonds for earthquakes in Mexico.

This thesis is organized as follows: chapter 2 presents an introduction of earthquakes, their characteristics, how they are measured and how the seismic risk can be transferred with financial instruments. Chapter 3 describes the definition of CAT bonds, their fundamentals, including their structure of cash flows, the trigger mechanisms and its comparison with default bonds and the reinsurance. It also offers their rating and some insights into the future of the CAT bonds market. Chapter 4 explains a real case, a parametric CAT bond for earthquakes that was sponsored by the Mexican government and issued in May 2006 by the special purpose CAT-MEX Ltd. The transaction was structured by Swiss Re AG and Deutsche Bank AG. In this chapter, the calibration of the bond is based on the estimation of the intensity rate that describes the earthquakes process from the two sides of the contract: from the reinsurance market that consists of the sponsor company (the Mexican government) and the issuer of reinsurance coverage (Swiss Re) and from the capital markets, which is formed by the issuer of the CAT bond (CAT-MEX Ltd.) and the investors. In addition, the historical intensity rate is computed. Once the intensity rates are estimated, a comparative analysis between the intensity

rates is conducted to know whether the Mexican government is buying reinsurance from Swiss Re at a fair price or whether Swiss Re is selling the bond to the investors for a reasonable price. The results demonstrate that Swiss Re estimates a probability of an earthquake lower than the one estimated from historical data. Under specific conditions, the financial strategy of the government, a mix of reinsurance and CAT bond is optimal in the sense that it provides coverage of $450 million for a lower cost than the reinsurance itself.

Since a modeled loss trigger mechanism takes other varibles into account that can affect the value of the losses, the pricing of a hypothetical CAT bond with a modeled loss trigger for earthquakes in Mexico is examined in chapter 5. Due to the missing information of losses, different loss models are proposed to describe the severity of earthquakes. In section 5.2 the analytical distribution is fitted to the loss data that is formed with actual and estimated losses. Section 5.3 presents different loss arrival point processes of natural events. This section describes that the homogenous Poisson process is the best process governing the flow of earthquakes. Formerly estimating the frequency and severity of earthquakes, the modeled loss is connected with an index CAT bond, using the compound doubly stochastic Poisson pricing methodology from Baryshnikov et al. (1998) and Burnecki and Kukla (2003). This methodology and Monte Carlo simulations are applied to the studied data to find the CAT bond prices for earthquakes in Mexico. The values of the zero and coupon CAT bonds associated to the modeled loss data, the threshold level and the maturity time are computed in section 5.4. Furthermore, the robustness of the modeled loss with respect to the CAT bond prices is analyzed. Because of the quality of the data, the results show that there is no significant impact of the choice of the modeled loss on the CAT bond prices. However, the expected loss is considerably more important for the evaluation of a CAT bond than the entire distribution of losses. The last part, chapter 6, provides a conclusion.

2 Seismology

Earthquakes can be generated by a sudden dislocation of large rock masses along fault lines fractures within the crust of the earth. Earthquakes can occur interplate or intraplate. Interplate earthquakes occur along their edges, where they may collide, slide past one another, or pull apart from another. Intraplate earthquakes transmit forces from the edges of the crustal plates that result in quakes in their interiors, Anderson et al. (1998).

The main parameters of an earthquake are its location, depth, fault rapture plane and magnitude. A quake starts at a single point, *the hypocenter*, and then propagates through a fault rupture plane. The area of this fault is an important determinant of the magnitude of the earthquake. The location of an earthquake, or the *epicenter*, is the initial point of rupture within the earth above the hypocenter. The *depth* is the distance between the hypocenter and the epicenter.

2.1 Earthquake magnitude

The magnitude of an earthquake can be defined as a numerical quantity of the total energy released. There are several magnitude scales, such as the moment magnitude, the surface wave magnitude, the body wave magnitude and the local (or Richter Mw) magnitude scales. These scales can be related to one another, Open File Report (1998).

The media often report earthquakes using the Richter scale. This scale was developed for a specific type of seismograph that is no longer in use. Richter magnitudes are local magnitudes, but do not imply a specific scale. The Richter magnitude scale compares the size of earthquakes in a mathematical way. The magnitude of an earthquake is determined from the logarithm of the amplitude and wave length (A/T) recorded by seismographs. On the Richter scale, the magnitude Mw is expressed in whole numbers and decimal fractions, where each whole number increase in magnitude represents a tenfold increase in measured amplitude; in terms of energy, each whole number in the magnitude scale corresponds to the release of about 31 times more energy than the amount associated with the preceding whole number value, USGS (2006).

2.2 Earthquake Intensity

The intensity of an earthquake is defined as the kind and amount of damage produced. It is measured with the Modified Mercalli scale (MMI), which is a numerical index describing the physical effects of an earthquake on man and man-built structures. MMI categories range from I to XII. The intensity at a given point depends not only on the strength of the earthquake (magnitude Mw) but also on the depth d and the local geology at that point. Table 2.1 shows the Modified Mercalli scale (MMI) and witness observations.

MMI scale	Witness observations
I	Felt by very few people; barely noticeable.
II	Felt by a few people, especially on upper floors.
III	Noticeable indoors, especially on upper floors, but may not be recognised as an earthquake. Hanging objects swing.
IV	Felt by many indoors, by few outdoors. May give the impression of a heavy truck passing by.
V	Felt by almost everyone, some people awakened. Small objects move. Trees and poles may shake.
VI	Felt by everyone. Difficult to stand. Some heavy items of furniture move, plaster falls. Slight damage to chimneys possible.
VII	Slight to moderate damage in well-built, ordinary structures. Considerable damage to poorly built structures. Some walls may fall.
VIII	Little damage in especially built structures. Considerable damage to ordinary buildings, severe damage to poorly built structures. Some walls collapse.
IX	Considerable damage to especially built structures, buildings shifted off foundations. Noticeable cracks in ground. Wholesale destruction.
X	Most masonry and frame structures and their foundations destroyed. Ground badly cracked. Landslides. Wholesale destruction.
XI	Total damage. Few, if any, structures standing. Bridges destroyed. Wide cracks in ground. Waves seen on ground.
XII	Total damage. Waves seen on ground. Objects thrown up into air.

Table 2.1: Modified Mercalli scale (MMI) and witness observations.
Source: USGS

2.3 Seismic Tools

The tools to register earthquakes are the seismograph and the accelerograph, which register the movement of the earth when a seismic wave passes. The seismograph can extend ten or hundred of thousand times the speed of the movement of the earth caused by a quake. When the seismic wave is very close to the seismograph, it shows a saturate seismogram and the wave cannot be registered. In this case the accerelograph is used. It registers the acceleration of the earth and is generally used to readjust the intensity of the quake movement on the seismograph.

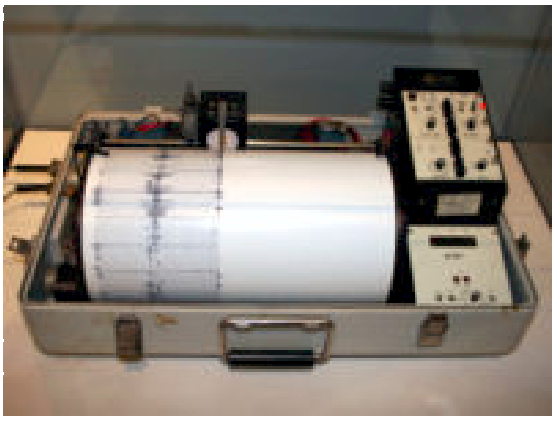

Figure 2.1: A seismograph used by the United States Department of Interior. Source: Wikipedia.

2.4 Location of epicenters

In order to find the accurate epicenter of an earthquake, it is necessary that many reporting stations calculate the distances from the epicenter to the stations. The arrival times of the seismic waves give a rough distance to the epicenter in kilometers, but do not give the direction. Once the reporting stations calculate the distances, the epicenter of the earthquake is given by the intersection point (E) of the circles from the different reporting stations. Figure 2.2 represents an earthquake in the coast of Guerrero, Mexico. It was registered in the reporting stations: Tacubaya, D.F. (TAC), Presa Infernillo, Mich. (PIM) and Pinotepa Nacional, Oax. (PIO), Suárez and Jiménez (1987). In practice, the procedure to localize the epicenter is more complicated, since the internal structure and sphere form of the earth should be considered.

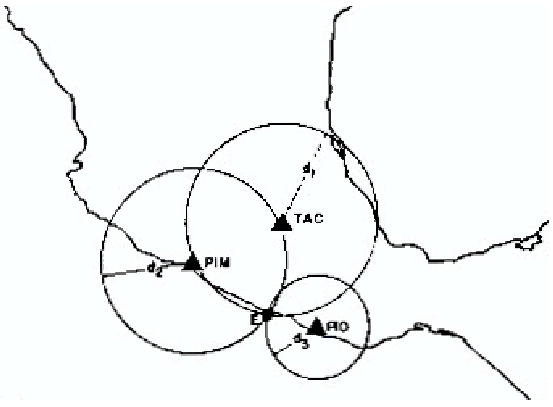

Figure 2.2: Location of earthquakes.

2.5 Seismology in Mexico

Mexico has a high level of seismic activity due to the interaction between the Cocos plate and the North American plate. The Central Guerrero segment, part of the Cocos Plate along the active subduction zone on Mexico's south western coast, is of great importance because it is a potential threat to Mexico City due to its proximity and lack of major activity since 1916. This zone along the Middle America Trench suffers large magnitude events with a frequency higher than any other subduction zone in the world. These events can cause substantial damage in Mexico City, due to a phenomenon known as the *Mexico City effect*. The Mexico City soil, which consists mostly of reclaimed, water-saturated lakebed deposits, amplifies 5 to 20 times the long-period seismic energy, RMS (2006). Due to this effect and the high concentration of exposure in Mexico City, seismic risk is on the top of the list for catastrophic risk in Mexico.

Historically, the Cocos plate boundary produced the 1985 Michoacan earthquake of magnitude 8.1 Mw Richter scale. It destroyed hundreds of buildings and caused thousand of deaths in Mexico City and other parts of the country. It is considered the most damaging earthquake in the history of Mexico City. The Mexican insurance industry officials estimated payouts of four billion dollars. In the last decades, other earthquakes have reached the magnitude 7.8 Mw Richter scale.

For earthquakes, the Mexican insurance market has traditionally been highly regulated, with limited protection provided to homeowners and reinsurance by the government. Today, after the occurrence of an earthquake, the reconstruction can be financed by transferring the risk to the capital markets with insurance linked securities (ILS) like catastrophic (CAT) bonds that would pass the risk on to investors or using the traditional reinsurance that would pass the risk on to reinsurers.

3 The catastrophic bonds

In the mid-1990's catastrophic bonds (CAT bonds), also named as *Act of God* or *Insurance-linked bond*, were developed to ease the transfer of catastrophic insurance risk from insurers, reinsurers and corporations (sponsors) to capital market investors.

3.1 Definition

CAT bonds are bonds whose coupons and principal payments depend on the performance of a pool or index of natural catastrophe risks, or on the presence of specified trigger conditions. They protect sponsor companies from financial losses caused by large natural disasters by offering an alternative or complement to traditional reinsurance.

CAT bonds provide risk transfer capacity for the sponsor's layer of risk that is often not reinsured because of its high severity and low frequency level. They supply protection without the risk of loss due to a counterparty defaulting on a transaction (credit risk).

CAT bonds usually have duration of one to five years, but the most common being three years. A multiyear term allows sponsors to prevent capacity at fixed costs, to anticipate risk management and portfolio changes and to amortize fixed costs over a period of years. For investors, a three years term bond avoids the reinvestment risk and effort of one year bonds, Clarke et al. (2005).

CAT bonds are multi peril o single peril bonds. While sponsors prefer to cover as many risks as possible in a single CAT bond offering to reduce transaction costs and share multiple territories, investors prefer single peril contracts for having possibilities to assemble a risk portfolio. Furthermore, they offer attractive returns and reduce the portfolio risk, since CAT bonds defaults are uncorrelated with defaults of other securities.

CAT bonds work like fully collateralized multi - year reinsurance contracts and are the major segment of the Insurance Linked Securities (ILS) market, Cizek et al. (2005).

3.2 Structure of Cash flows - Timing

The transaction involves four parties: the sponsor or ceding company (government agencies, insurers, reinsurers), the special purpose vehicle SPV (or issuer), the collateral and the investors (institutional investors, insurers, reinsurers, and hedge funds). The basic structure is shown in Figure 3.1. It can be summarized as follows:

- Sponsor sets up a SPV as an issuer of the bond and a source of reinsurance protection. The SPV is typically structured as a Cayman Islands (whose common shares are held by a charitable trust) for a remote bankruptcy.
- The issuer sells bonds to capital market investors and the proceeds are deposited in a collateral account, in which earnings from assets are collected and from which a floating rate is payed to the SPV.
- The sponsor enters into a reinsurance or derivative contract with the issuer and pays him a premium.
- The SPV usually gives quarterly coupon payments to the investors. The premium that the ceding company pays for the insurance coverage, and the investment bond proceeds that the SPV received from the collateral, are a source of interest or coupons paid to investors.
- If there is no trigger event during the life of the bonds, the SPV gives the principal back to the investors with the final coupon or the generous interest. But if the specific catastrophic risk is triggered, the SPV pays the ceding according to the terms of the reinsurance contract and sometimes pays nothing or partially the principal and interest to the investors.

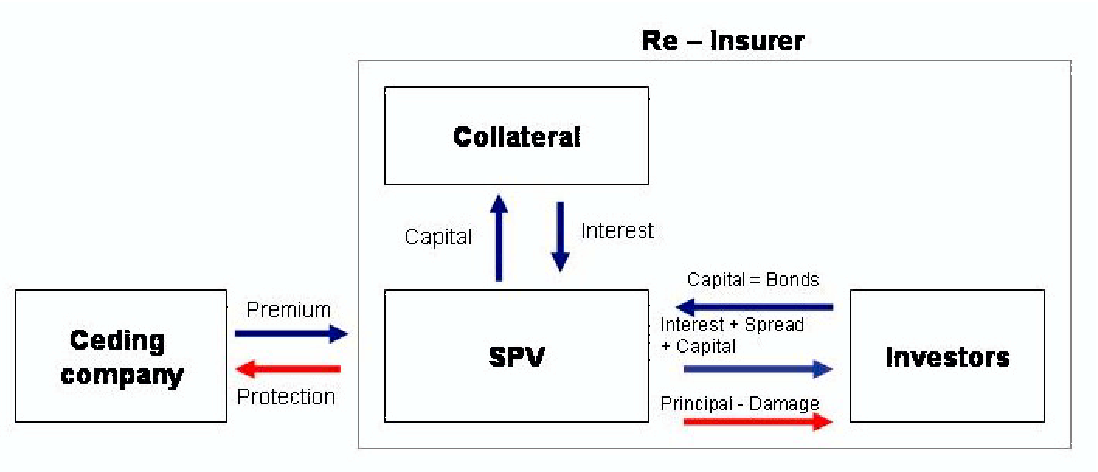

Figure 3.1: CAT bond cash flows diagram. In case of event (red arrow), no event (blue arrow)

3.3 Types Trigger mechanism

There is a variety of trigger mechanisms to determine when the losses of a natural catastrophe should be covered by the CAT bond. These include the indemnity, the industry index, the pure parametric, the parametric index and the modeled loss trigger. Figure 3.2 shows a range of levels of basis risks and transparency to investors offered by each of these mechanisms.

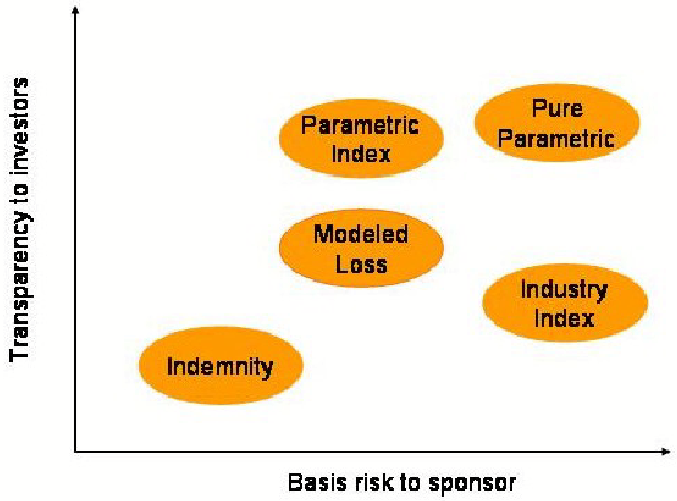

Figure 3.2: Trigger mechanisms. Source: Dubinsky (2005).

3.3.1 Indemnity trigger

The indemnity trigger involves the actual loss of the ceding company. The ceding company receives reimbursement for its actual losses from the covered event, above the predetermined level of losses. It has no basis risk, i.e. there is no risk that, in the event of a covered loss, the payout determined by the bond calculation will differ from the actual loss incurred by the sponsor. This trigger closely replicates the traditional reinsurance, but it is exposed to catastrophic and operational risk of the ceding company.

Additionally, the indemnity trigger faces asymmetric information problems as adverse selection, moral risk and not fully information access. There is adverse selection, when the ceding company tries to keep the most profitable parts of a portfolio and gives up the unprofitable ones. The moral risk rises when the ceding company modifies its underwriting policies or there is an increase in its claim payments at the expenses of a reduction in the coupon or principal value of the investors, Anderson et al.(1998). For example, in May 2003 the indemnity multi peril CAT bond called *Residential Re 2003 Ltd.* was issued by U.S.A.A Reinsurance with a value of $160 million for three years coverage, Dubinsky and Laster (2005).

3.3.2 Industry index trigger

With an industry index trigger, the ceding company recovers a proportion of total industry losses in excess of a predetermined point to the extent of the remainder of the principal. The ceding company is exposed to basis risk, since its own losses differs from that of the industry. An industry index trigger allows the ceding company to avoid detailed information disclosure to competitors and makes a transparent deal to investors when an independent party reports the industry loss, for example the Property Claim Services (PCS) in the United States of America. In addition to the adverse selection and moral hazard, it has an extended development period to determined coverage. Transactions based on the industry index trigger follow one of the next three approaches: parametric, industry loss or modeled loss.

An example of this trigger is the *SR Earthquake Fund* CAT bond. It was issued by Swiss Re in July 1997, with a value of $137 million for two years coverage of earthquake risk in California.

3.3.3 Pure parametric index trigger

The parametric index payouts are triggered by the occurrence of a catastrophic event with certain defined physical parameters, for example wind speed and location of a hurricane or the magnitude or location of an earthquake. It is transparent to investors and has a shorter development period, but it is subject to basis risk when the geographical distribution of the ceding company's book of business differs from that of the CAT bond.

The *Parametric Re* is an example of a parametric CAT bond. Its value was of $100 million and was issued by Tokyo Marine in November 1997 to cover earthquake risk in Tokyo for ten years.

3.3.4 Parametric index trigger

The Parametric index trigger uses different weighted boxes to reflect the ceding company's exposure to events in the area. Data from the parameters of the catastrophic event is collected at multiple reporting stations and then entered into specified formulas, which track losses of the ceding company's portfolio. For example a Hurricane Index value is defined as, Dubinsky and Laster (2005):

$$K \sum_{i=1}^{I} w_i (v_i - L)^n$$

where K and n are constants, i is the relevant location, I is the total number of locations, w_i indicates the weight of the location i defined in the contract, v_i is the calculated peek gust wind speed at location i and L is a constant representing the threshold peek gust wind speed above which a damage exist. The Hurricane index is the sum of the storm damage at each location weighted by predefined location weights, which reflect the ceding company's exposure at each location. The index value determines the loss payout.

An example of this trigger is the *PIONEER 2003 II-B* CAT bond with a value of $12 million to cover wind for three years in Europe. It was issued by Swiss Re in June 2003.

3.3.5 Modeled loss trigger

After a catastrophe occurs the physical parameters of the catastrophe are used by a modelling firm to estimate the expected losses to the ceding company's portfolio. Instead of dealing with the company's actual claims, the transaction is based on the estimates of the model. If the modeled losses are above a specified threshold, the bond is triggered. For investors, this trigger is less transparent since they cannot see through the framework of the modelling firm. This trigger offers a short payout period. In June 2001 Zurich Reinsurance issued a three year modeled loss CAT bond *Trinom*, for $162 million to cover multi peril, Clarke et al. (2006).

3.4 Default bonds and CAT bonds

There is a similarity between default bonds prices and CAT bonds prices. In order to price a default bond the partial or complete loss of the principal value should be considered. Default bonds yield high returns, partly due to their potential default ability. CAT bonds yield high returns because of the unpredictable nature of the process of catastrophes. However, a difference between the CAT bonds and the high yield bonds is the information flow and the price processes. In a high yield bond the information about the issuer arrives constantly, while the information about a natural event is available only after it occurs. Whereas defaulting high yield bond prices are affected by business cycles and corporate events, CAT bond prices stay as a function of the expected loss calculation.

3.5 Rating

CAT bonds are often rated by an agency such as Standard & Poor's (S&P), Moody's, or Fitch Ratings. Typically, a corporate bond is rated based on its probability of bankruptcy. A CAT bond is rated based on its probability of default due to a natural event like an earthquake or a hurricane, triggering loss of the principal. Standard & Poor's focus is on attachment probability, Moody's focus is on the expected loss and Fitch's focus combines both the attachment probability and the expected loss. Many CAT bonds are rated BB+ by S&P, which is just below investment grade but better than non-investment grade, IAIS (2003).

3.6 Comparison against reinsurance

In the reinsurance, the insurance companies transfer their own portfolio risk to other reinsurance companies that manage their risk by a broader diversification. In an *excess of loss (XOL)* reinsurance contract, the reinsurance provides the ceding company with protection against a layer of losses above a certain level, in exchange for the payment of a premium. In a *proportional* reinsurance contract, the reinsurance provides capital on a proportional sharing basis, i.e. the ceding company is reimbursed for a fixed percentage of its losses in return for ceding a fixed percentage of premiums.

From the sponsor perspective, the CAT bonds exhibit facts that can be compared with the reinsurance. These include, Dubinsky and Laster (2005):

- The CAT bond price is relative according to the insurance underwriting cycle. Reinsurance prices are very volatile after the occurrence of a catastrophe. In these times, when the industry capital has short supply, the insurance industry increases rates in order to rebuild surplus. However in times of excess capacity, insurers lower rates, making CAT bond prices less attractive.
- In terms of line of catastrophe business, reinsurance has the ability to diversify among many non-peak perils, whose prices are low because of their low capital charge (the amount of capital a reinsurer must hold per amount of coverage limit provided). For peak perils, CAT bonds and reinsurance may have comparable pricing due to the high capital charge.
- Whereas CAT bonds provide fixed costs coverage over a multi-year period, insurers hedge the exposure of increasing rates for homeowners multi peril coverage by entering into a reinsurance contract, whose rates may be expensive in the market.
- While the reinsurance can give rises to coverage and payment disagreements, CAT bonds offer a systematic claim procedure, i.e. unambiguous payment terms. Thereby the CAT bonds minimize the loss development period.
- CAT bonds minimize the counterparty risk that can arise with the traditional reinsurance. For the reinsurance part of the CAT bond, the SPV invests the collateral in a high rated investment. The collateral's default probability is uncorrelated with the occurrence of the natural catastrophes.
- CAT bonds are attractive surplus alternatives. They can cover multiple perils over multi year terms and can respond easier to capital structure than the reinsurance. The structure of the CAT bonds keeps the transaction off the issuers's balance sheet.

From the investor perspective, CAT bonds also offer advantages, Dubinsky and Laster (2005):

- CAT bonds have paid returns significantly in excess of return on corporate bonds with similar credit rating and maturities. Besides, as long as the CAT bonds are not triggered, the bonds give coupon payments to investors.

- CAT bonds are a source of diversification. The CAT bonds risk shows no correlation with the risk of corporate bonds or equities. Adding a CAT bond into a portfolio reduces the portfolio risk, without changing the expected return. Hence, the risk - return profile improves in a portfolio.
- The impact of adverse credit events on the CAT bonds is reduced. The CAT bond market may be vulnerable to catastrophic events in the insurance and reinsurance market, but not to widespread corporate defaults.

3.7 Pricing CAT bonds

The evaluation of a CAT bond is affected by several variables. The CAT bond pricing involves the analysis of the underlying risk exposure, including the expected loss and the likelihood of different scenarios. One can estimate the risk of a natural catastrophe, using simulations of significant catastrophic events. From the simulated events, an *artificial loss experience* can be constructed to calculate the expected loss of a CAT bond. Modelling results are the main drivers of bond ratings and the bond price can be determined by looking at bonds with similar rating.

3.8 Market Prospects

During the period 1997 - 2005, Guy Carpenter and MMC Securities Corporation reported that 69 catastrophe bonds have been issued with total risk limits of $10.65 billion, whose predominant sponsors were insurers and reinsurers. The CAT bond market has increased in the number and variety of investors. The secondary market liquidity has perhaps improved due to the increase of the size of individual peril issues and the growth in bonds outstanding, Clarke et al. (2006).

Today, the catastrophe bond market features a increasing *know-how* that has helped investors and sponsors to move along the learning curve. The cost of issuance of CAT bonds has lowered thanks to reduction of coupons and transaction expenses, making CAT bonds more competitive with the reinsurance market. In spite of the market has suffered the first loss to a publicly disclosed CAT bond with the hurricane Katrina in 2005, the ILS market is optimistic to achieve a beyond growth trend of the CAT bond, Mooney (2005) and Clarke et al. (2006).

4 The Mexican parametric CAT Bond

In order to reduce the exposure of Mexico to the impact of natural catastrophes and to recover quickly as soon as they occur, the government established the Mexico's Fund for Natural Disasters (FONDEN) in 1996. In the presence of disaster, the FONDEN's operational basics establish that local governments can declare a situation of emergency to get resources immediately from the fund to mitigate the effects, SHCP (2001).

Since its creation this fund has suffered from problems of political economy. The contributions to the fund have been reduce since 2001. Before, there have been some years of low collection of taxes, causing no contributions to the fund. The FONDEN's resources have been insufficient to meet the government's obligations.

Faced with the shortage of the FONDEN's resources and the high probability of earthquake occurrence, the Mexican government decided to issue a parametric CAT bond against earthquake risk. The decision was taken because the instrument design protects and magnifies, with a degree of transparency, the resources of the trust. The CAT bond payment is based on some physical parameters of the underlying event (e.g. the magnitude Mw), thereby there is no justification of losses. The parametric CAT bond helps the government with emergency services and rebuilding after a big earthquake. Moreover the CAT bond avoids the credit risk from the reinsurance, since the capital raised by issuing the CAT bond is invested in safe securities, which are held by a special purpose vehicle (SPV).

In this chapter, the calibration of this parametric CAT bond is based on the estimation of the probability of earthquake from the two different parts of the CAT bond contract: from the reinsurance market and the capital market. In addition, the probability of earthquake is computed from historical data. As the probability of earthquakes depends on its intensity rate that describes the flow process of earthquakes, one estimates the intensity rate from the reinsurance market λ_1, from the capital markets λ_2 and from historical data λ_3. Once the intensity rates are estimated, a comparative analysis between them is conducted to know whether the Mexican government was fairly buying insurance from Swiss Re or whether the latter was selling the bond to investors at a reasonable price.

4.1 Issue

In May 2006, the Mexican government has sponsored the first parametric CAT bond for earthquakes in Mexico. It was issued by a special purpose Cayman Islands CAT-MEX Ltd. and structured by Swiss Re AG and Deutsche Bank AG. The $160 million CAT bond pays a tranche equal to the London Inter-Bank Offered Rate (LIBOR) plus 230 basis points, see Table 4.1. The CAT bond is part of a total coverage of $450 million provided by Swiss Re for three years against earthquake risk and with total premiums of $26 million. The government hired Air Worldwide Corporation to model the seismic risk and which detected nine seismic zones, see Figure 4.1. Given the federal governmental budget plan, just three out of these nine zones were defined in the transaction: zone 1, zone 2 and zone 3, with coverage of $150 million in each case, SHCP (2004).

Issue Date	May-06
Sponsor	Mexican government
SPV	CAT-Mex Ltd
Reinsurer	Swiss Re
Total size	$160 million
Risk Period	3 year
Risk	Earthquake
Structure	Parametric
Spread	LIBOR plus 230 basis points

Table 4.1: Parametric Mexican CAT bond

The CAT bond payment would be triggered if there is an *event*, i.e. an earthquake higher or equal than 8 Mw hitting zone 1 or zone 2, or an earthquake higher or equal than 7.5 Mw hitting zone 5, see Table 4.2.

Zone	Threshold u in $Mw \geq$ to:
Zone 1	8
Zone 2	8
Zone 5	7.5

Table 4.2: Thresholds u's of the Mexican parametric CAT bond

The cash flows diagram for the mexican CAT bond are described in Figure 4.2. CAT-MEX Ltd. is a special purpose Cayman Islands whose ordinary shares are held in charitable trust. It issues the bond that is placed among investors, who receive interests and get the principal back if there is no earthquake of certain strength. CAT-MEX Ltd. invests the proceeds in high quality assets within a collateral account. Simultaneous to the issuance of the bond, CAT-MEX Ltd. enters into a reinsurance contract with Swiss Re. The premium and the proceeds are used to make the coupon payments to the bondholders. In case of occurrence of a trigger event, an earthquake with a certain magnitude in any of the three defined zones in Mexico, Swiss Re pays

the covered insured amount to the government, which stops paying premiums at that time and investors sacrifices their full principal and coupons.

The proceeds of the bond will serve to provide Swiss Re coverage for earthquakes in Mexico in connection with an insurance agreement that Swiss Re has entered into with the Natural Disasters Fund of Mexico.

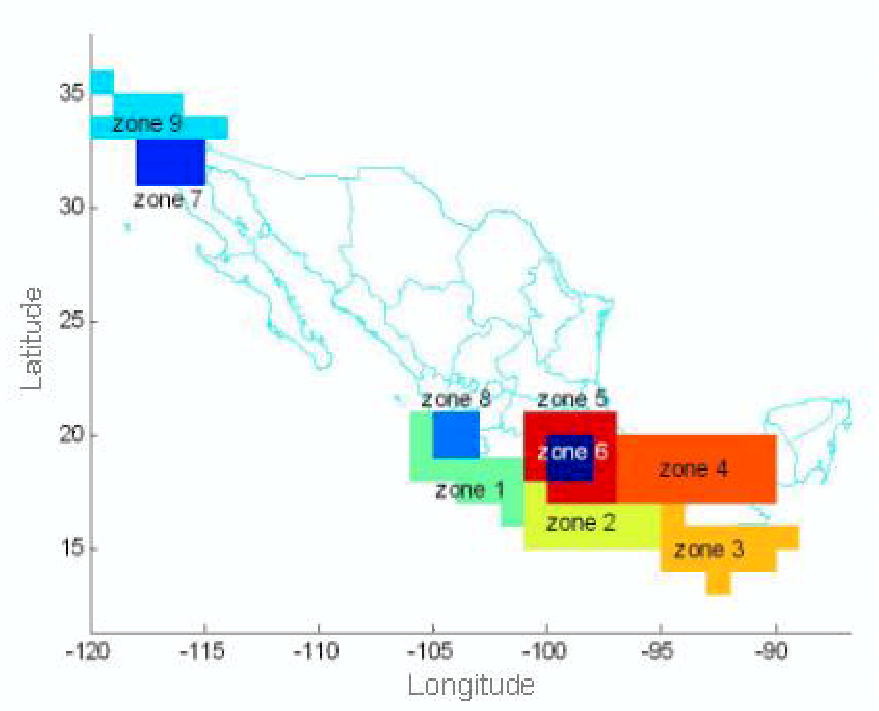

Figure 4.1: Map of seismic regions in Mexico. Source: SHCP

4.2 Calibrating the Mexican CAT bond

Assuming perfect financial market, where there are no arbitrage opportunities, no transaction costs, no taxes, and no restrictions on short selling, Franke et al. (2000), the calibration of the parametric CAT bond is based on the estimation of the intensity rate that describe the flow process of earthquakes.

Let $(\Omega, \mathcal{F}, \mathcal{F}_t, P)$ be a probability space and $\mathcal{F}_t \subset \mathcal{F}$ an increasing filtration, with time $t \in [0, T]$. The arrival process of earthquakes or the number of earthquakes in the interval $(0, t]$ is described by the process $N_{t\geq 0}$. This process uses the times T_i when the ith earthquake occurs or the times between earthquakes $W_i = T_i - T_{i-1}$. The earthquake process N_t in terms of W_i's is defined as:

$$N_t = \sum_{n=1}^{\infty} I_{(T_n < t)} \tag{4.1}$$

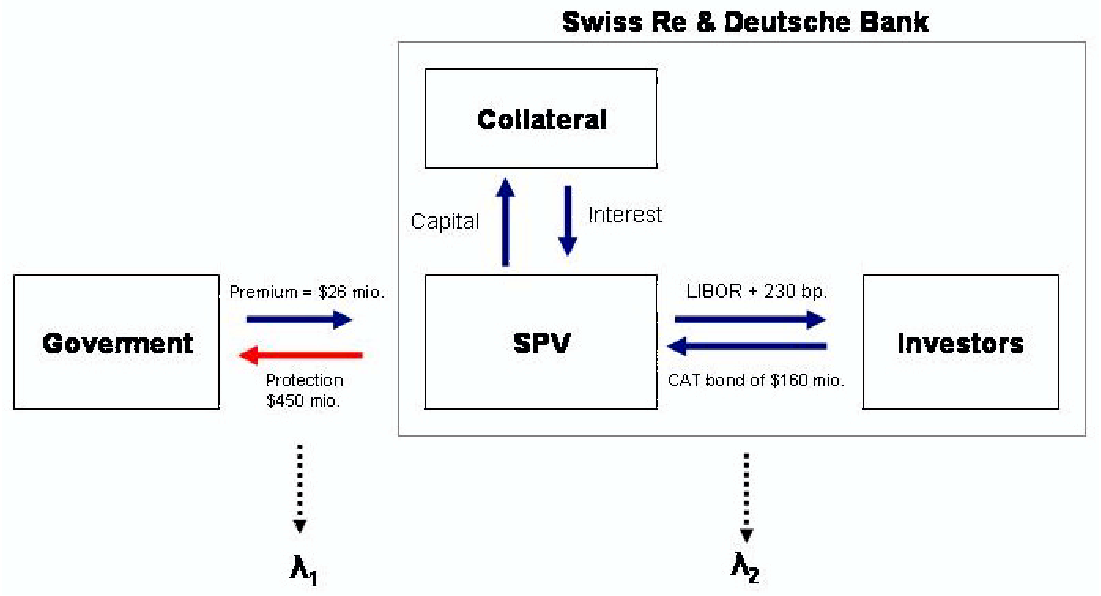

Figure 4.2: Cash flows diagram of the Mexican CAT bond. In case of event (red arrow), no event (blue arrow).

Since earthquakes can strike at any time during the year with the same probability, they suffer the *loss of memory property* $\mathrm{P}(X > x + y | X > y) = \mathrm{P}(X > x)$, where X is a random variable. The arrival process of earthquakes $N_{t:t\geq 0}$ can be characterized with a Homogeneous Poisson Process (HPP), with intensity rate $\lambda > 0$ if, Cizek et al. (2005):

- N_t is a point process governed by the Poisson law.
- The waiting times $W_i = T_i - Ti - 1$ are independent identically and exponentially distributed with intensity λ.

The probability of no occurrence of an earthquake in the interval $(0, t]$ is given by:

$$\mathrm{P}(W_i \geq t) = e^{-\lambda t}$$

Hence, the probability of occurrence of an earthquake is:

$$\mathrm{P}(W_i < t) = 1 - \mathrm{P}(W_i \geq t) = 1 - e^{-\lambda t}$$

with density function:

$$f(t) = \lambda e^{-\lambda t} \tag{4.2}$$

where intensity rate $\lambda > 0$.

To calibrate the parametric CAT bond, the probabilities of earthquake and the corresponding intensity rates describing the flow process of earthquakes are estimated from the two sides of the contract: from the reinsurance and the capital markets. These estimations are based

on actuarial principles. In addition the intensity rate from the historical data is computed and based on the *intensity model*, which is developed later in this chapter. Define λ_1 as the intensity rate of the process of earthquakes from the reinsurance transaction part of the Mexican parametric CAT bond, λ_2 be the intensity rate from the financial part and λ_3 be the intensity rate from historical data.

4.2.1 Insurance market intensity: λ_1

Assume a flat term structure of interest rates and consider a process of continuously compounded discount interest rates. Let H and J be random variables with values at time t and density functions $f(h)$ and $f(j)$ respectively. Denote H as the government's payoff or the annually premiums that the government pays to Swiss Re for the three years reinsurance contract $T = 3$. Let J represent the Swiss Re's payoff to the government or the covered insured amount in case of occurrence of an event over a three year period. Additionally, assume that the arrival process of earthquakes follows a HPP with intensity λ_1.

Suppose that the non-arbitrage condition holds, a compounded discount *actuarially fair insurance price* at time $t = 0$ is:

$$\mathrm{E}\left[He^{-tr_t}\right] = \mathrm{E}\left[Je^{-tr_t}\right] \tag{4.3}$$

i.e. the insurance premiums are equal to the value of the expected loss from earthquake, where:

$$\mathrm{E}\left[He^{-tr_t}\right] = \int_0^T he^{-tr_t}\lambda_1 e^{-\lambda_1 t}dt$$

and

$$\mathrm{E}\left[Je^{-tr_t}\right] = \int_0^T je^{-tr_t}\lambda_1 e^{-\lambda_1 t}dt$$

Notice that the expectations above involve the occurrence probability of the insured event. From the given information, the total premium value $\mathrm{E}\left[He^{-tr_t}\right] = \$26$ million and the covered insured amount j is equal to \$450 million. Assume that the annual continously compounded discount interest rate is $r = \ln(1 + r_t) = 5.35\%$, constant and equal to the London Inter-Bank Offered Rate (LIBOR) in June 2006, FannieMae (2006). Substituting these values in equation (4.3), it follows:

$$26 = \int_0^3 450\lambda_1 e^{-t(r_t+\lambda_1)}dt \tag{4.4}$$

where $1 - e^{-\lambda_1 t}$ is the probability of occurrence of an earthquake. Hence, solving the nonlinear equation (4.4), one estimates the intensity rate from the reinsurance market λ_1 equal to 0.0215. That means that the premium paid by the government to Swiss Re considers a probability of occurrence of an event in three years equal to 0.0624. In other words, Swiss Re expects 2.15 events in one hundred years.

4.2.2 Capital market intensity: λ_2

The contract structure defines a coupon CAT bond, which pays to the investors the principal P at time to maturity $T = 3$ and gives coupons C every 3 months during the bond's life in case of no event. If there is an event, the investors sacrifice their principal and coupons. These coupon bonds pay a fixed spread s over LIBOR. The spread rate s that CAT-MEX Ltd. offers to investors is equal to 230 basis points over LIBOR. The LIBOR is assumed to be $r = 5.35\%$ in June 2006, FannieMae (2006). The principal or the initial investors payoff from the bond purchase is equal to $P = \$160$ million. The fixed coupons payment C have a value (in \$ million) of:

$$C = \left(\frac{r+s}{4}\right) P = \left(\frac{5.35\% + 2.3\%}{4}\right) 160 = 3.06 \tag{4.5}$$

Let G be a time dependent random variable that defines the investors' gain from investing in the bond, which consists of the principal and coupons. Consider that the annual discretely compounded discount interest rate is $r_t = e^r - 1 = 5.5\%$, where r is the annual continuously compounded discount interest rate LIBOR equal to $r = 5.35\%$. Moreover, assume that the arrival process of earthquakes follows a HPP with intensity λ_2. In the non-arbitrage framework, a discretely discount *fair bond price* at time $t = 0$ is given by:

$$P = \mathrm{E}\left[G\left(\frac{1}{1+r_t}\right)^t\right] \tag{4.6}$$

where

$$\mathrm{E}\left[G\left(\frac{1}{1+r_t}\right)^t\right] = \sum_{t=1}^{12}\left(\frac{1}{1+r_t}\right)^{\frac{t}{4}} Ce^{-\lambda_2 \frac{t}{4}} + \left(\frac{1}{1+r_t}\right)^T Pe^{-\lambda_2 T}$$

In this case, the investors receive 12 coupons during 3 years and its principal P at maturity $T = 3$. Hence, substituting the values of the principal $P = \$160$ million and the coupons $C = \$3.06$ million in equation (4.6), it follows:

$$160 = \sum_{t=1}^{12} 3.06\left(\frac{e^{-\lambda_2}}{1+r_t}\right)^{\frac{t}{4}} + \frac{160e^{-3\lambda_2}}{(1+r_t)^3} \tag{4.7}$$

Solving the equation (4.7), the intensity rate from the capital market λ_2 is equal to 0.0222. In other words, the capital market estimates a probability of occurrence of an event equal to 0.0644, equivalently to 2.22 events in one hundred years.

4.2.3 Historical Intensity: λ_3

Additionally to the estimation of the intensity rate for the reinsurance and the capital markets, the historical intensity rate that describes the flow process of earthquakes λ_3 is calculated. The data was provided by the National Institute of Seismology in Mexico (SSN). It describes the time t, the depth d, the magnitude Mw and the epicenters of earthquakes higher than 6.5 Mw

occurred in the country from the year 1900 to 2003. Table 4.3 shows some descriptive statistics for the variables time t, depth d and magnitude Mw of the earthquake historical data that considers 192 observations.

Descriptive	t	d	Mw
Minimum	1900	0	6.5
Maximum	2003	200	8.2
Mean	1951	39.54	6.9
Median	1950	33	6.9
Variance		1573.69	0.14
Sdt. Error		39.66	0.37
25% Quantile		12	6.6
75% Quantile		53	7.1
Skewnewss		1.58	0.92
Kurtosis		5.63	3.25
Excess		2.63	0.25
Nr. obs.	192	192	192
Distinct obs.	82	54	18

Table 4.3: Descriptive statistics for the variables time t, depth d and magnitude Mw of the 1900-2003 earthquake data.

The frequency of the magnitude Mw of earthquakes of the historical data is displayed in Table 4.4. Notice that earthquakes less than 6.5 Mw were not taken into account because of their high frequency and low loss impact.

Mw	Frequency	Percent	% Cumulative
6.5	30	16%	16%
6.6	21	11%	27%
6.7	28	15%	41%
6.8	14	7%	48%
6.9	22	12%	60%
7	18	9%	69%
7.1	12	6%	76%
7.2	7	4%	79%
7.3	8	4%	83%
7.4	9	5%	88%
7.5	6	3%	91%
7.6	9	5%	96%
7.7	1	1%	96%
7.8	3	2%	98%
7.9	1	1%	98%
8	1	1%	99%
8.1	1	1%	100%
8.2	1	1%	100%

Table 4.4: Frequency of the magnitude Mw for the 1900-2003 earthquake data

Table 4.5 shows the frequency of the zones where the earthquakes have occurred. Almost 50% of the earthquakes has occurred in the insured zones, mainly in zone 2. This confirms the high earthquake activity in these zones.

Zone	Frequency	Percent	% Cumulative
1	30	16%	16%
2	42	22%	38%
5	18	9%	47%
Other	102	53%	100%

Table 4.5: Frequency of the earthquake location for the 1900-2003 earthquake data

Let Mw_i be independent and identically distributed random variables, indicating the magnitude Mw of the ith earthquake at time t. The estimation of the historical λ_3 is based on the *intensity model*. This model assumes that there exist independent identically random variables ϵ_i, called *trigger events*, that characterize earthquakes with magnitude Mw_i higher than a defined threshold u.

Recalling again the fact that the arrival process of earthquakes follows a Poisson process N_t with intensity $\lambda > 0$, whose times between earthquakes W_i are exponentially distributed with intensity λ, a new process B_t is defined to characterize the trigger event process:

$$B_t = \sum_{i=1}^{N_t} I_{\{\epsilon_i\}} = \sum_{i=1}^{N_t} I_{\{Mw_i \geq u\}} \tag{4.8}$$

where N_t is the Poisson process describing the number of earthquakes. B_t is a process which counts only earthquakes that trigger the CAT bond's payoff. However, the dataset contains only three such events, what leads to the calibration of the intensity of B_t based on only two waiting times. Therefore in order to compute λ_3, consider the process B_t and define p as the probability of occurrence of a trigger event conditional on the occurrence of the earthquake. Then the probability of no event up to time t is given by:

$$\begin{aligned}
\mathrm{P}(B_t = 0) &= \mathrm{P}(N = 0) + \mathrm{P}(N_t = 1)(1-p) + \mathrm{P}(N_t = 2)(1-p)^2 + \dots \\
&= \sum_{k=0}^{\infty} \mathrm{P}(N_t = k)(1-p)^k \\
&= \sum_{k=0}^{\infty} \frac{(\lambda t)^k}{k!} e^{(-\lambda t)} (1-p)^k \\
&= \sum_{k=0}^{\infty} \frac{(\lambda(1-p)t)^k}{k!} e^{(-\lambda t)} e^{-\lambda(1-p)t} e^{\lambda(1-p)t}
\end{aligned}$$

by definition of the Poisson distribution function and since,

$$\sum_{k=0}^{\infty} \frac{(\lambda(1-p)t)^k}{k!} e^{-\lambda(1-p)t} = 1$$

then

$$\mathrm{P}(B_t = 0) = e^{-\lambda p t} = e^{-\lambda_3 t} \tag{4.9}$$

Now the calibration of the λ_3 can be decomposed into the calibration of the intensity of all earthquakes with a magnitude higher than 6.5 Mw and the estimation of the probability of the trigger event.

As mentioned before, in the historical data three out of 192 earthquakes are identified as trigger events within the insured zones, i.e. their magnitude Mw was higher than the defined thresholds u's in Table 4.2 and which were defined by the modelling company. The probability of occurrence of the trigger event is equal to $p = \left(\frac{3}{192}\right)$. The estimation of the annual intensity is obtained by taking the mean of the daily number of earthquakes times 360 i.e. $\lambda = (0.005140)(360)$ equal to 1.8504. Consequently the annual historical intensity rate for a trigger event is equal to $\lambda_3 = \lambda p = 1.8504\left(\frac{3}{192}\right) = 0.0289$. In other words, approximately 2.89 events are expected to occur in the designated areas of the country within one hundred years. Table 4.6 displays the date, the zone and the magnitude Mw of the three trigger events.

Year	Mw	Zone
1957	7.8	5
1985	8.1	1
1995	8	1

Table 4.6: Trigger events occurred in the insured zones

Table 4.7 summarizes the values of the intensities rates λ's and the probabilities of occurrence of a trigger event in one and three years. Whereas the reinsurance market expects 2.15 events to occur in one hundred years, the capital market anticipates 2.22 events and the historical data predicts 2.89 events. Observe that the value of the λ_3 depends on the time period of the historical data. The intensity rate $\lambda_3 = 0.0289$ is estimated from the years 1900 to 2003 and it is not very accurate since it is based on three events only. For a different period, λ_3 might be smaller than λ_1 or λ_2.

	λ_1	λ_2	λ_3
Intensity	0.0215	0.0222	0.0289
Probability of event in 1 year	0.0212	0.0219	0.0284
Probability of event in 3 year	0.0624	0.0644	0.0830
No. expected events in 100 years	2.1555	2.2223	2.8912

Table 4.7: Calibration of intensity rates: the intensity rate from the reinsurance market λ_1, the intensity rate from the capital market λ_2 and the historical intensity rate λ_3. CMXCMktInt.xpl CMXRMktInt.xpl

The magnitude of earthquakes above 6.5 Mw that occurred in Mexico during the years 1990 to 2003 are illustrated in Figure 4.3. It also indicates the earthquakes that occurred in the insured zones and those whose magnitude were higher than the defined thresholds u's by the modelling company. The three trigger events are identified with filled circles.

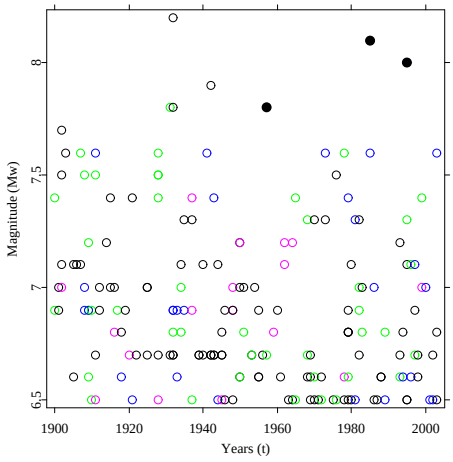

Figure 4.3: Magnitude of trigger events (filled circles), earthquakes in zone 1 (black circles), earthquakes in zone 2 (green circles), earthquakes in zone 5 (magenta circles), earthquakes out of insured zones (blue circles)

CMX01.xpl

Apparently the difference between the intensity rates λ_1, λ_2 and λ_3 seems to be insignificant, but for the government it has a financial and social repercussion since the intensity rate of the flow process of earthquakes influences the price of the parametric CAT bond that will help the government to obtain resources after a big earthquake.

The small difference between the intensity rates λ_1 and λ_2 might be explained by the absence of the public and liquid market of earthquake risk in the reinsurance market, just limited information is available. This might cause the pricing in the reinsurance market to be less transparent than pricing in the capital markets. Another reason why the intensity rate λ_2 is higher than the intensity rate λ_1 might be because contracts in the capital market are more expensive than contracts in the reinsurance market. This is assumed because the cost of risk capital (the required return necessary to make a capital budgeting project) in the capital markets is higher than that in the reinsurance market. Moreover the reinsurance contract might be less expensive than the CAT bond because of the associated risk of default. A CAT bond presents no credit risk as the proceeds of the bond are held in a SPV (CAT-Mex Ltd.), a transaction off the Swiss Re's balance sheet.

The differences between the intensity rates λ_1 and λ_3 or λ_2 and λ_3 could be explained by the

presence of just three trigger events in the historical data. The estimation of λ_3 is not very precise since it is based on the time period of the historical data. A different period could lead to a lower historical intensity rate. The accuracy of λ_3 plays an important role when one considers it as a reference intensity rate. It involves different interpretations about the calibration of the parametric CAT bond.

One could expect that risk adverse companies that insure against the largest catastrophic losses could pay higher prices, since the reinsurance market imperfections might explain the differences between theory and observed insurer behaviour. Froot (1999) considers that the reinsurance market suffers from a shortage of capital, particularly after a catastrophic event occurred. Scarce capital would give reinsurance firms the ability to gain more market power that will enable them to charge higher premiums than expected.

Supposing that λ_3 would be the real intensity rate describing the flow of process of earthquakes, the results in Table 4.7 demonstrate that, contrary to the theory predictions, the Mexican government paid total premiums of \$26 million that is 0.75 times the real actuarially fair one (\$34.49 million), which is obtained by substituting the historical intensity $\lambda_3 = 0.0289$ in equation (4.4), that is:

$$\int_0^3 450\lambda_3 e^{-t(r_t+\lambda_3)}dt = 34.49$$

At first glance, it appears that either the government saves \$8.492 million (\$34.3million - \$26 million) in transaction costs from transferring the seismic risk with a reinsurance contract or that Swiss Re is underestimating the occurrence probability of a trigger event. This is not a valid argument because the actuarially fair reinsurance price assumes that the coverage payout depends only on the loss of the insured event. In reality, the reinsurance market and the coverage payouts are exposed to other risks, such as the credit risk, that can affect the value of the premium. Considering this fact, the probability that Swiss Re will default over the next three years could be approximately equal to the price discount that the Government gets in the risk transfer of earthquake risk ($\frac{\leq \$8.492}{\$26} \leq 32.6\%$).

Another explanation of the low premiums for covering the seismic risk might be the mix of the reinsurance contract and the CAT bond. Since the \$160 million CAT bond is part of a total coverage of \$450 million, the reinsurance company transfers 35% of the total seismic risk to the investors, who effectively are betting that a trigger event will not hit specified regions in Mexico in the next three years. If there is no event, the money and interests are returned to the investors. If there is an event, Swiss Re must pay to the government \$290 million from the reinsurance part and \$160 million from the CAT bond to cover the insured loss of \$450 million. The value of the premium for \$290 million coverage with intensity rate λ_1 is:

$$\int_0^3 290\lambda_1 e^{-t(r_t+\lambda_1)}dt = 16.751$$

Then the total premium of \$26 million that the government pays to Swiss Re to get a coverage of \$450 million in case of a trigger event might consist of \$16.751 million premium from the reinsurance part and the CAT bond and \$9.245 million (\$26 million - \$16.751 million) for

transaction costs or the management added value or for coupon payments. The proceeds of the bond that are invested in high quality assets and part of the premium are used to pay the coupons.

Under the assumption that the intensity rate λ_3 would be the real intensity rate describing the flow process of earthquakes, the financial strategy of the government, a mix of reinsurance and CAT bonds is optimal in the sense that it provides coverage of \$450 million against seismic risk for a lower cost than the reinsurance itself, which has an actuarially fair premium equal to \$34.49 million. However, this financial strategy of the government does not eliminate completely the costs imposed by market imperfections.

5 Pricing modeled loss CAT bonds for earthquakes in Mexico

In this chapter, under the assumptions of non-arbitrage and continuous trading, the pricing of a modeled loss CAT bond for earthquakes is examined. The importance of a modeled loss trigger mechanism is that it takes other variables into account that can affect the value of the losses, for example not only considers the magnitude Mw of the earthquake, but also the depth d, impact on cities, etc. Besides, the payout of the bond will be based on historical and estimated losses. The pricing methodology is based on the article of Barishnikov et al. (1998) and Burnecki and Kukla (2003). In order to determine the CAT bond prices, they modelled the stochastic process underlying the CAT bond as a compound doubly stochastic Poisson process. An application of their results is conducted to the Mexican earthquake data from the National Institute of Seismology in Mexico (SSN) and to its corresponding loss data that was built by López (2003). In particular, the key drivers of the CAT bonds pricing are studied: the frequency and severity of earthquakes.

In section 5.1 the loss data set and its adjustments are discussed. Section 5.2 presents different loss models, the use of the EM algorithm to treat the missing data and the estimation of the distribution functions which fit the modeled loss in a suitable form. In section 5.3, different arrival processes of earthquakes are examined. This section reveals that the homogenous Poisson process is the best process governing the flow of earthquakes, whose intensity rate λ is estimated in the previous chapter. Section 5.4 introduces the compound doubly stochastic Poisson pricing methodology from Baryshnikov et al. (1998) and Burnecki and Kukla (2003). This methodology together with Monte Carlo simulations is applied to the studied data to find the prices of zero and coupon CAT bonds for earthquakes in Mexico. The values of bonds are associated to the modeled loss data, the threshold level and the expiration time. In order to check how robust the modeled loss with respect to the CAT bond prices is, Monte Carlo simulations are used once more.

5.1 Data

In the past, Mexico did not have specialized institutions which could quantify the losses caused by earthquakes. Empirical studies are conducted to the loss data that López (2003) built for the earthquakes, which were obtained from the National Institute of Seismology in Mexico (SSN). The historical losses of earthquakes occurred in Mexico during the years 1900 - 2003 were adjusted to the population growth, the inflation and the exchange rate (peso/dollar) and were converted to USD of 1990. The annual Consumer Price Index (1860-2003) was used for the inflation adjustment and the Average Parity Dollar-Peso (1821-1997) was used for the exchange rate adjustment, both provided by the U.S. Department of Labour. For the population adjustment, the annual population per Mexican Federation (1900-2003) provided by the National Institute of Geographical and Information Statistics in Mexico (INEGI) was used, López (2003).

Table 5.1 describes some descriptive statistics for the variable time t, depth d, magnitude Mw and adjusted loss X of the historical data. From 1900 to 2003, the data considers 192 earthquakes higher than 6.5 Mw and 24 of them with financial adjusted losses.

The adjusted losses in million US dollar and the corresponding magnitude Mw of earthquakes occurred in Mexico are illustrated in Figure 5.1. The peaks mark the occurrence of the 8.1 Mw earthquake in 1985 and the 7.4 Mw earthquake in 1999. The earthquake in 1932 had the highest magnitude in the historical data (8.2 Mw), but its losses are not big enough compared to the other earthquakes.

Descriptive	t	d	Mw	X ($ million)
Minimum	1900	0	6.5	10.73
Maximum	2003	200	8.2	0
Mean	1951	39.54	6.93	1443.69
Median	1950	33	6.9	0
Variance	-	1573.69	0.14	11060.5
Sdt. Error	-	39.66	0.37	105.16
25% Quantile	1928	12	6.6	0
75% Quantile	1979	53	7.1	0
Skewnewss	-	1.58	0.92	13.19
Kurtosis	-	5.63	3.25	179.52
Excess	-	2.63	0.25	176.52
Nr. obs.	192	192	192	192
Distinct obs.	82	54	18	24

Table 5.1: Descriptive statistics for the variables time t, depth d, magnitude Mw and loss X of the loss historical data

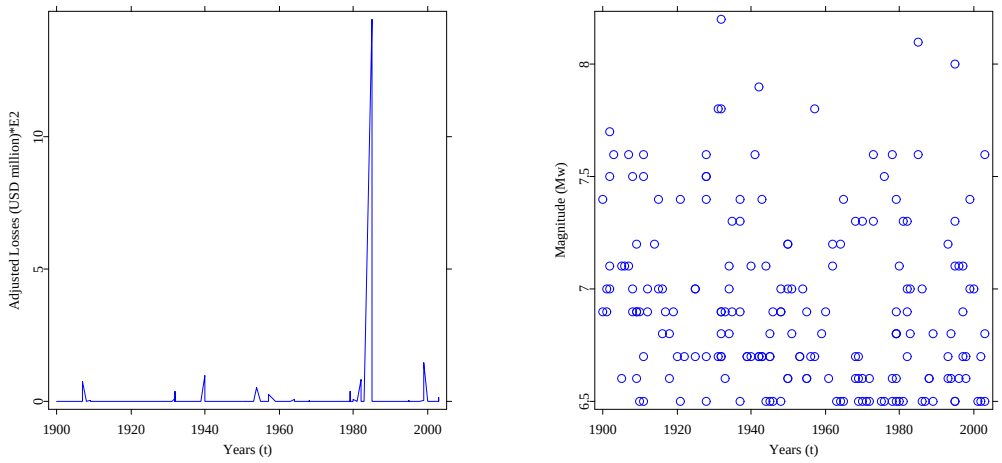

Figure 5.1: Plot of adjusted Losses (left panel) and the magnitude Mw (right panel) of earthquakes occurred in Mexico during the years 1900-2003.

CMX02.xpl

5.2 Earthquake severity

Let $(\Omega, \mathcal{F}, \mathcal{F}_t, P)$ be a probability space and $\mathcal{F}_t \subset \mathcal{F}$ an increasing filtration representing the history of the past and present of some underlying finance process, with time $t \in [0, T]$. Let $\{X_k\}_{k=1}^{\infty}$ be independent and identically random variables characterizing the loss severities caused by earthquakes. In this section the modelling of the loss severity of earthquakes is studied.

5.2.1 Modeled loss

In order to predict future losses, the use of historical loss data is very problematic, because of the disproportional population growth within seismic areas and the change of the properties value, building materials and construction designs. A modeled loss trigger mechanism considers other variables that affect the value of the losses, for example it takes the physical characteristics of the earthquakes into account.

Earthquake losses can be affected by several variables such as the magnitude Mw, the depth d of the earthquake or by dummy variables, for example whether the earthquake had impact on Mexico City (the most important zone in the country). Experts in geography describe that the earthquake losses are directly proportional to the magnitude Mw and inversely proportional to the depth of the earthquake, Rosenblueth (2000).

The scatter plots in Figure 5.2 show the relationships of the adjusted losses X_k (vertical axis) of the historical data with respect to the variable magnitude Mw, depth d and the dummy indicator of the earthquake impact on Mexico City $I_{(0,1)}$. The data reports that 15.6% of the earthquakes had impact on the country's capital. Since the data includes two outliers or two observations that are away from the mean value see Figure 5.1, the scatter plots in Figure 5.3 exclude the 8.1 Mw earthquake in 1985 and in Figure 5.4 the scatter plots do not consider the 8.1 Mw earthquake in 1985 and the 7.4 Mw earthquake in 1999. Note that when all the historical adjusted losses are considered, they are directly proportional to the time t and the magnitude Mw, and inversely proportional to the depth d. However, when the outliers are excluded, the adjusted losses are inversely proportional to the time, magnitude and depth. This reflects the importance of the outliers. The 1985 earthquake of 8.1 Mw had payouts of four billion dollars or its equivalent adjustment of 1443.69 million dollars. When this outlier is eliminated, the relationship between the adjusted losses and the variables time t and magnitude Mw changes.

Once observing the relationships between the variables in the scatter plots, the approach to get the estimated loss is by means of the linear regression that is defined as, Härdle and Simar (2003):

$$x = \alpha + \beta_1 y_{i1} + \ldots + \beta_p y_{ip} + \epsilon_i; i = 1, \ldots, n. \tag{5.1}$$

where $x(n \times 1)$ is a vector of observations on the response variable, $y(n \times p)$ is a data matrix on the p explanatory variables, α is the intercept, β_i with $i = 1 \ldots n$ are the coefficients of the variables and ϵ_i the errors.

The linear regression loss models in Table 5.2 are applied to the historical earthquake loss data. Since losses are positive and greater than zero, $X_k \geq 0$, the dependent variable in the linear regression models is the natural logarithm of the loss $\ln(X)$. The independent variables are the magnitude Mw, the logarithm of the magnitude $\ln(Mw)$, the depth d, the dummy indicator of the earthquake impact on Mexico City $I_{(0,1)}$ and interactions of variables, like $Mw \cdot d$ or $\ln(Mw)d$. Notice in Table 5.2 that the logarithm of the depth $\ln(d)$ is not used, as the depth d of an earthquake can be zero.

The criterion to select the best modeled loss is given by the highest coefficient of determination r^2, which describes the percentage of the explained variation over the total variation, Härdle and Simar (2003):

$$r^2 = \frac{\sum_{t=1}^{n}(\hat{x}_i^2 - \bar{x})^2}{\sum_{t=1}^{n}(x_i^2 - \bar{x})^2} \tag{5.2}$$

where $\hat{x}_i$ is the predicted value and $\bar{x}$ is the mean of the values x_i. Table 5.2 display the coefficients of determination for each of the proposed linear regresion models of the historical adjusted loss data r^2_{LR1}. It also provides the coefficients of determination for the data without the observation of the earthquake in 1985 r^2_{LR2} and for the data without the outliers of the earthquakes in 1985 and 1999 r^2_{LR3}. Observe that the dummy variable $I_{(0,1)}$ has no significant impact on the loss models 6 and 22, 7 and 24, 9 and 25.

The standard errors are also estimated for each of the loss models of the historical adjusted loss data (SE_{LR1}), for the case without the outlier of the earthquake in 1985 (SE_{LR2}) and for the case without the outliers of the earthquakes in 1985 and 1999 (SE_{LR3}). Table 5.3 shows the standard errors (SE) that are defined as:

$$SE(\hat{\beta}) = Var(\hat{\beta})^{\frac{1}{2}} = \frac{\sigma}{(n \cdot s_{YY})^{\frac{1}{2}}} \tag{5.3}$$

where $\hat{\beta}$ is the coefficients estimator, n is the number of variables and s_{YY} is the empirical covariance matrix.

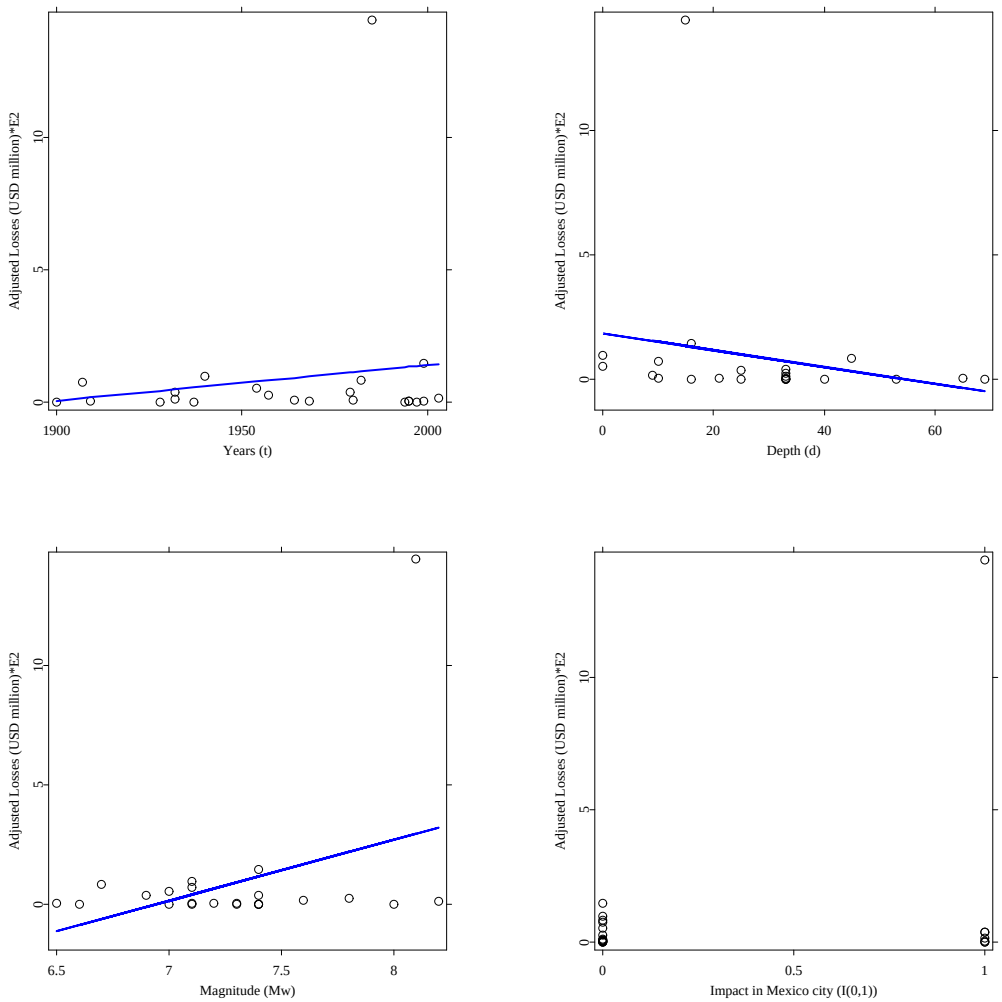

Figure 5.2: Plot of adjusted losses with the time t, the depth d (Upper panel), the magnitude Mw and the dummy variable $I_{(0,1)}$ (Lower panel)

CMX031.xpl

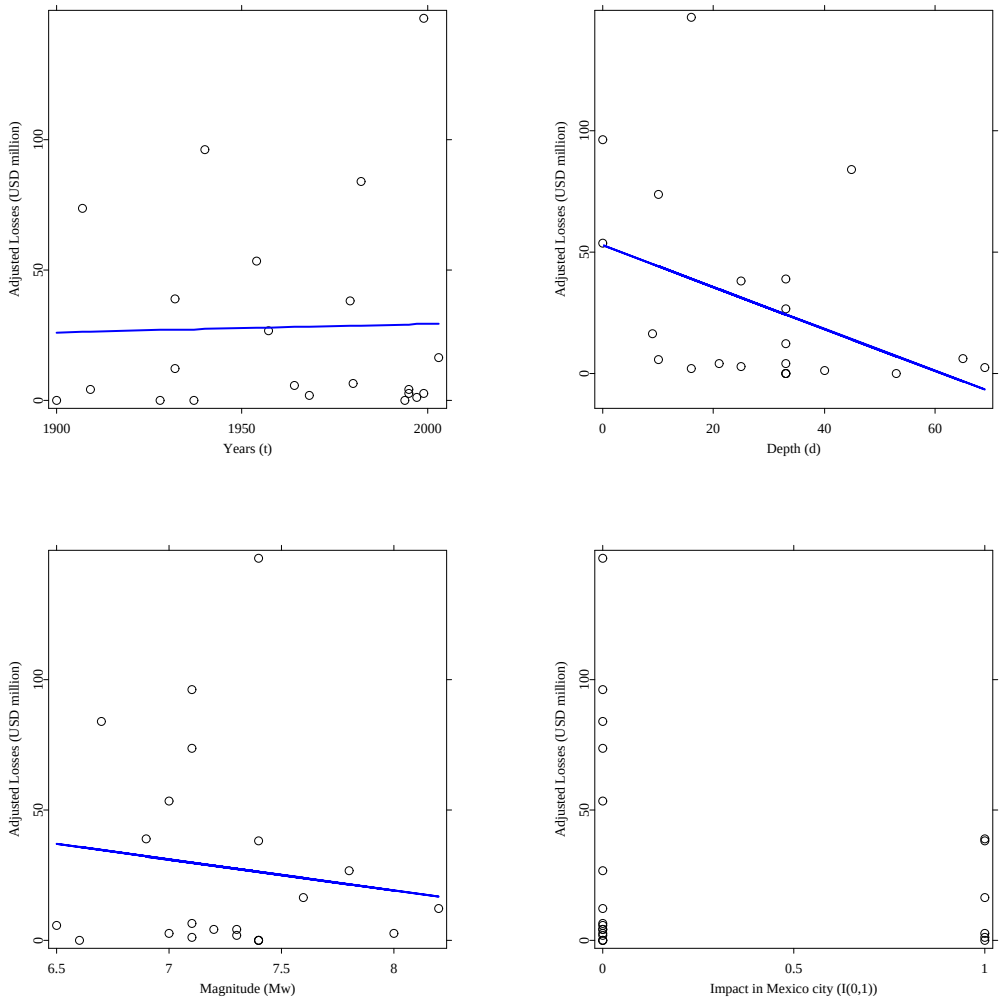

Figure 5.3: Plot of adjusted losses with the time t, the depth d (Upper panel), the magnitude Mw and the dummy variable $I_{(0,1)}$ (Lower panel), without the outlier of the 1985 earthquake.

CMX032.xpl

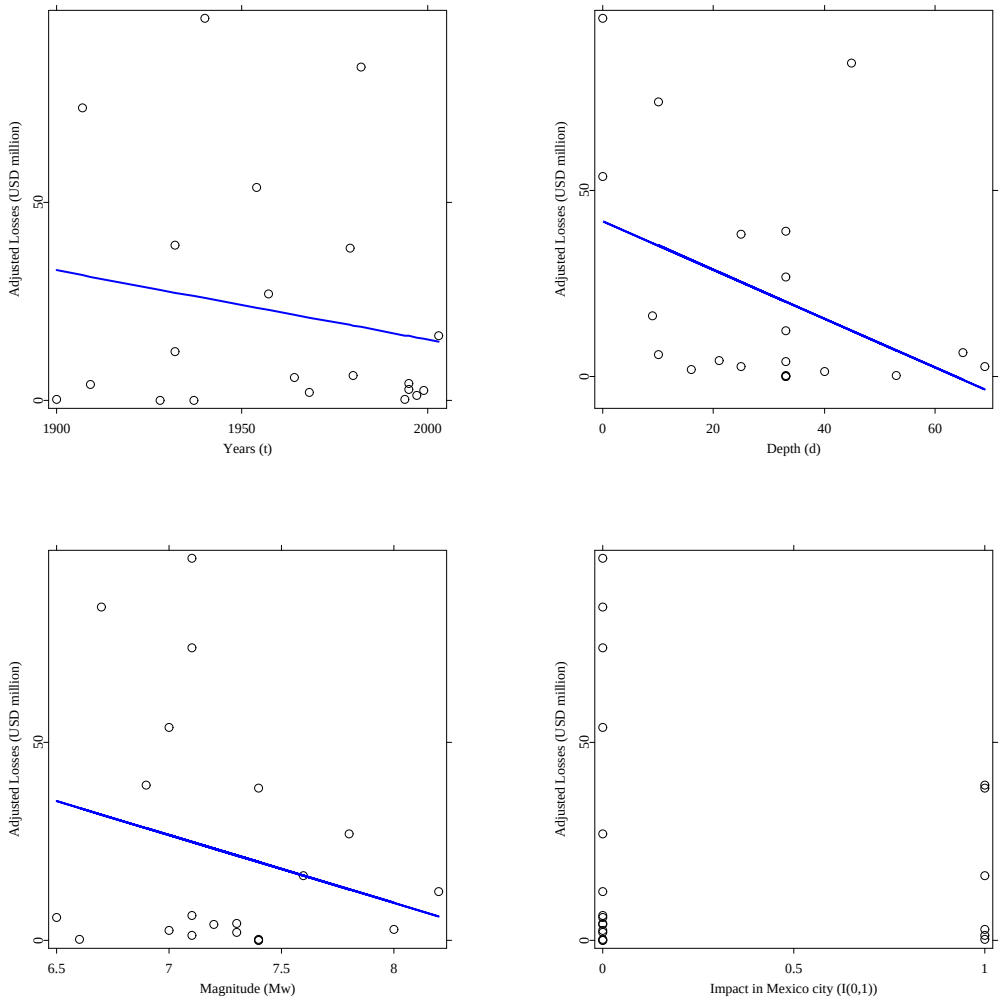

Figure 5.4: Plot of adjusted losses with the time t, the depth d (Upper panel), the magnitude Mw and the dummy variable $I_{(0,1)}$ (Lower panel), without the outliers of the 1985 & 1999 earthquakes

CMX033.xpl

Model	y	x_1	x_2	x_3	x_4	r^2_{LR1}	r^2_{LR2}	r^2_{LR3}
1	$\ln(x)$	Mw				0.015	0.002	0.004
2	$\ln(x)$	$\ln(Mw)$				0.013	0.002	0.005
3	$\ln(x)$		d			0.151	0.130	0.111
4	$\ln(x)$	Mw	d			0.154	0.138	0.123
5	$\ln(x)$	$\ln(Mw)$	d			0.153	0.138	0.125
6	$\ln(x)$	Mw	d		$Mw \cdot d$	0.220	0.147	0.127
7	$\ln(x)$	$\ln(Mw)$	d		$Mw \cdot d$	0.210	0.146	0.126
8	$\ln(x)$	Mw	d		$\ln(Mw) \cdot d$	0.225	0.150	0.129
9	$\ln(x)$	$\ln(Mw)$	d		$\ln(Mw) \cdot d$	0.216	0.148	0.128
10	$\ln(x)$	Mw		$I_{(0,1)}$		0.028	0.002	0.006
11	$\ln(x)$	$\ln(Mw)$		$I_{(0,1)}$		0.027	0.002	0.007
12	$\ln(x)$		d	$I_{(0,1)}$		0.170	0.130	0.115
13	$\ln(x)$			$I_{(0,1)}$	$Mw \cdot d$	0.172	0.137	0.121
14	$\ln(x)$			$I_{(0,1)}$	$\ln(Mw) \cdot d$	0.171	0.134	0.118
15	$\ln(x)$	Mw	d	$I_{(0,1)}$		0.171	0.139	0.127
16	$\ln(x)$	$\ln(Mw)$	d	$I_{(0,1)}$		0.170	0.139	0.128
17	$\ln(x)$	$\ln(Mw)$	d	$I_{(0,1)}$	$Mw \cdot d$	0.210	0.146	0.128
18	$\ln(x)$	Mw		$I_{(0,1)}$	$\ln(Mw) \cdot d$	0.174	0.140	0.128
19	$\ln(x)$	$\ln(Mw)$		$I_{(0,1)}$	$\ln(Mw) \cdot d$	0.173	0.140	0.129
20	$\ln(x)$		d	$I_{(0,1)}$	$Mw \cdot d$	0.172	0.144	0.128
21	$\ln(x)$		d	$I_{(0,1)}$	$\ln(Mw) \cdot d$	0.172	0.145	0.129
22	$\ln(x)$	Mw	d	$I_{(0,1)}$	$Mw \cdot d$	0.220	0.148	0.128
23	$\ln(x)$	Mw	**d**	$I_{(0,1)}$	$\ln(Mw) \cdot d$	**0.226**	**0.151**	**0.129**
24	$\ln(x)$	$\ln(Mw)$	d	$I_{(0,1)}$	$Mw \cdot d$	0.210	0.146	0.128
25	$\ln(x)$	$\ln(Mw)$	d	$I_{(0,1)}$	$\ln(Mw) \cdot d$	0.216	0.149	0.129

Table 5.2: Coefficients of determination of the linear regression models applied to the adjusted loss data (r^2_{LR1}), without the outlier of the earthquake in 1985 (r^2_{LR2}) and, without the outliers of the earthquakes in 1985 and 1999 (r^2_{LR3})

Under the selection criterion, the highest r^2 is equal to 0.2260 and it corresponds to the model number 23:

$$\ln(x) = -27.99 + 2.10Mw + 4.44d - 0.15I_{(0,1)} - 1.11\ln(Mw) \cdot d$$

For the case without the outlier of the earthquake in 1985, the highest r^2 is equal to 0.1510 and it corresponds to the model number 23:

$$\ln(x) = -7.38 + 0.97Mw + 1.51d - 0.19I_{(0,1)} - 0.52\ln(Mw) \cdot d$$

For the case without the outliers of the earthquakes in 1985 and 1999, the highest r^2 is equal to 0.1299, which also corresponds to the model number 23:

$$\ln(x) = 1.3037 + 0.4094Mw + 0.2375d + 0.1836I_{(0,1)} - 0.2361\ln(Mw) \cdot d$$

Observe that the estimated regression coefficients are very sensitive to outliers. The estimated earthquake losses generated by the best modeled loss, number 23, are plotted in Figure 5.5.

Model	SE_{LR1}	SE_{LR2}	SE_{LR3}
1	2.9970	2.8289	2.7853
2	2.9996	2.8286	2.7844
3	2.7817	2.6414	2.6314
4	2.8452	2.6972	2.6853
5	2.8466	2.6960	2.6834
6	2.8036	2.7559	2.7580
7	2.8213	2.7582	2.7584
8	2.7941	2.7517	2.7546
9	2.8105	2.7543	2.7557
10	3.0506	2.9024	2.8590
11	3.0526	2.9020	2.8580
12	2.8192	2.7090	2.6986
13	2.8159	2.6977	2.6883
14	2.8165	2.7027	2.6928
15	2.8903	2.7698	2.7573
16	2.8911	2.7686	2.7554
17	2.8986	2.8379	2.8398
18	2.8849	2.7677	2.7565
19	2.8861	2.7668	2.7548
20	2.8890	2.7612	2.7559
21	2.8880	2.7592	2.7537
22	2.8802	2.8352	2.8407
23	**2.8698**	**2.8302**	**2.8383**
24	2.8986	2.8379	2.8398
25	2.8875	2.8335	2.8384

Table 5.3: Standard errors of the linear regression models applied to the adjusted loss data (SE_{LR1}), without the outlier of the earthquake in 1985 (SE_{LR2}) and without the outliers of the earthquakes in 1985 and 1999 (SE_{LR3})

EM algorithm

Since 23 out of 192 observations have information about earthquake losses, it is necessary to treat the missing data of losses for a further analysis. An approach to deal with the missing data is the Expectation - Maximum algorithm (EM). This algorithm consists of omitting the cases with missing data and running a regression on what remains. The regression coefficient will be used to estimate the missing data. After this *estimation step*, a new regression will be done over the complete data (including estimated values). With the new regression coefficients, the missing data is re-estimated. This process will continue until the estimates are adjusted to a given model sampling error, i.e. there is not longer a noticeable change. This is called the *maximization step*.

The solution from the EM algorithm is better than the elimination of the missing data, but it will still underestimate the standard errors of the coefficients. There are other alternatives that will be better than the ones obtained by the EM algorithm, but they assume a distribution of

the variables with missing data (usually the multivariate normal distribution), Howell (1998).

To fill the missing data of losses, the EM algorithm with linear regression was applied to the estimated loss datas of the best loss models (number 8, 22, 23, 24 and 25) and to the historical adjusted loss data. An interesting result is that after applying 1000 iterations and a given sampling error of 0.002, the algorithm converges fairly rapidly, meaning that the estimated coefficients do not show up a significant change from one iteration to another.

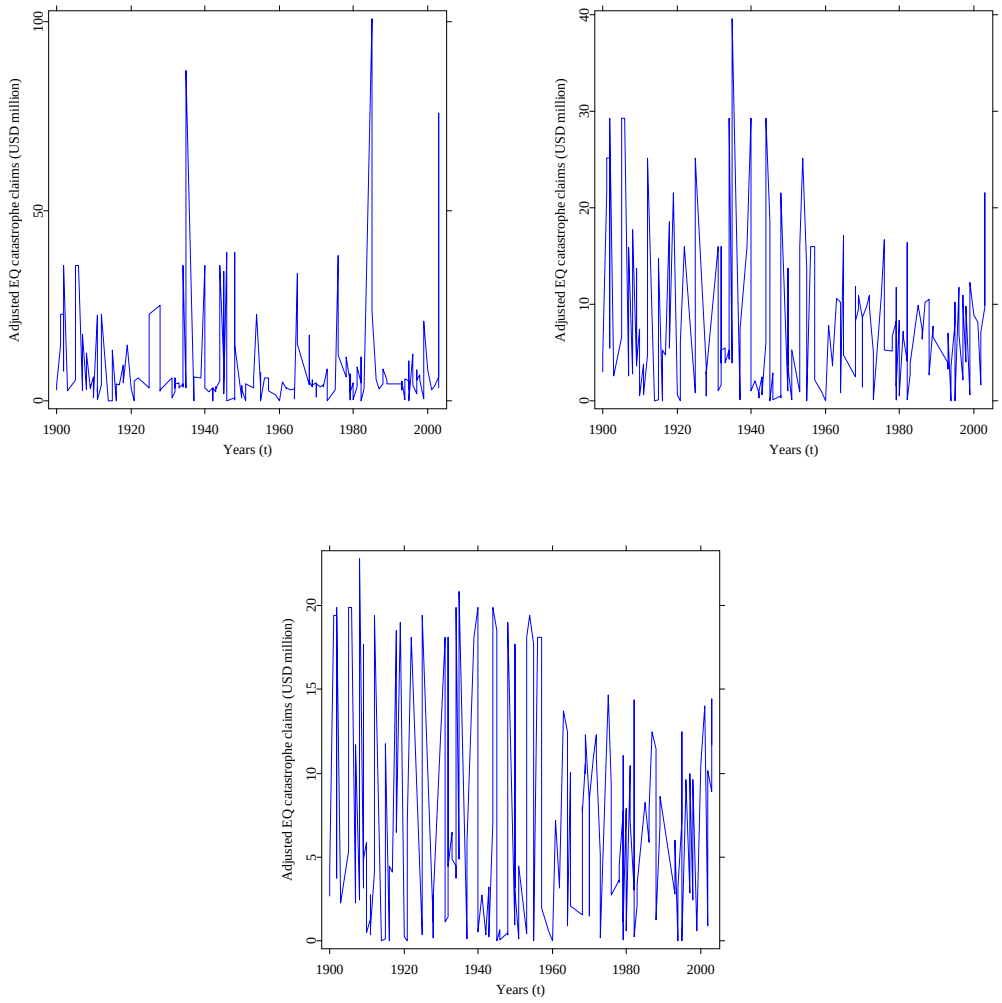

Figure 5.5: Modeled losses of earthquakes occurred in Mexico during 1990-2003 (upper left panel), without the outlier of the earthquake in 1985 (upper right panel) and without the outliers of the earthquakes in 1985 and 1999 (lower panel)

CMXmyEMalgorithm.xpl

Table 5.4 describes the descriptive statistics for the historical adjusted loss data, for the esti-

mated loss data obtained with the best linear regression model (number 23) and for the mix of historical with estimated loss data using the EM algorithm. The same procedure is applied for the case without the outliers of 1985 and 1999. Considering the importance of the historical data, from now on the loss data of earthquakes in Mexico considers historical and estimated losses.

Descriptive	HL_1	EL_1	HEL_1	HL_2	EL_2	HEL_2	HL_3	EL_3	HEL_3
Minimum	0.00	0.00	0.00	0.00	0.00	0.00	0.00	0.00	0.00
Maximum	1443.69	100.70	1443.69	146.54	39.59	146.54	96.32	22.79	96.32
Mean	10.7309	8.68	17.56	3.23	7.83	10.14	2.47	7.12	8.91
Median	0.00	4.30	4.30	0.00	5.30	5.43	0.00	4.54	4.90
Variance	11060.50	180.16	11022	254.87	59.23	268.01	12.12	43.49	159.86
Sdt. Error	105.17	13.42	104.99	15.96	7.70	16.37	146.97	6.59	12.64
25% Quantile	0.00	2.95	2.95	0.00	2.46	2.20	0.00	1.49	1.25
75% Quantile	0.00	7.94	8.14	0.00	10.66	10.97	0.00	11.03	12.22
Skewnewss	13.19	3.87	13.07	6.25	1.43	4.78	5.84	0.77	3.93
Kurtosis	179.53	21.94	177.36	46.32	4.79	33.16	38.66	2.25	23.58
Excess	176.53	18.94	174.36	43.32	1.79	30.16	35.66	-0.75	20.58
Nr. obs.	192	192	192	191	191	191	190	190	190
Diff. obs.	24	129	137	23	128	136	22	127	135

Table 5.4: Descriptive statistics for the historical adjusted losses (HL_1), estimated losses (EL_1), historical-estimated losses (HE_1) of the modeled loss number 23, without the outlier of earthquake in 1985 (HL_2, EL_2, HEL_2) and without the outliers of the earthquakes in 1985 and 1999 (HL_3, EL_3, HEL_3)

Figure 5.6 depicts the historical and estimated losses caused by earthquakes, given in million dollars, for the modeled loss number 23. The peaks of the picture on the upper left panel remark the occurrence of the earthquake in September 1985 and September 1999. Their influence is notably important.

5.2.2 Loss Distribution

The lack of past data or missing information about losses and other data for risk analysis make the derivation of the loss distribution from catastrophic natural events data a difficult task. In this subsection, the derivation of the distribution of losses caused by earthquakes is covered, using the empirical, the analytical and the moment approach. The mean excess function, the Goodness of fit and the limited expected value function help to find the accurate analytical loss distribution.

Empirical Method

When there is a large volume of data, the empirical method is the most appropriate approach to find the analytical loss distribution. In this method a smooth estimate of the cumulative

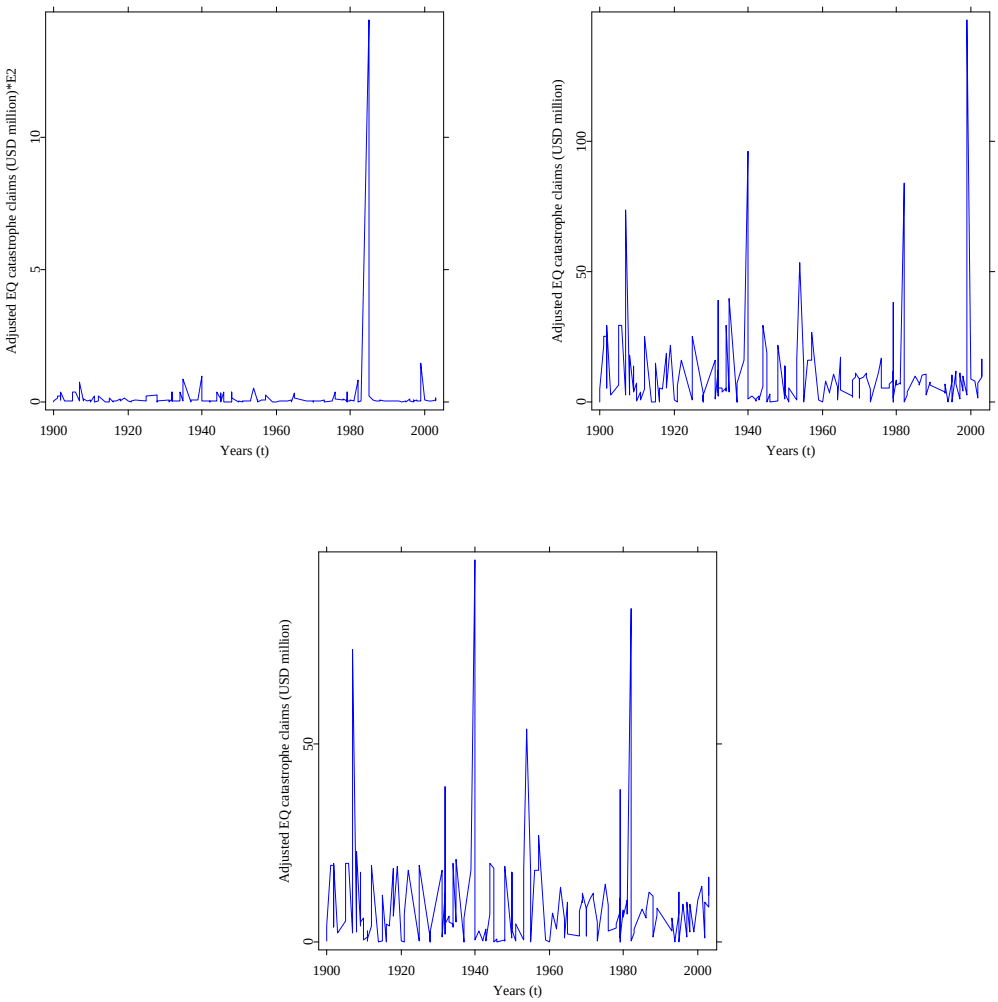

Figure 5.6: Historical and modeled losses of earthquakes occurred in Mexico during 1990-2003 (upper left panel), without the outlier of the earthquake in 1985 (upper right panel), without outliers of the earthquakes in 1985 and 1999 (lower panel)

CMXmyEMalgorithm.xpl

distribution function (cdf) is attained. For a sample of observation $x_1, ..., x_n$ the empirical distribution function (edf) is a piecewise constant function with jumps of size $\frac{1}{n}$ at points x_i. It is defined as:

$$F_n(x) = \frac{1}{n}\#i : x_i \leq x \tag{5.4}$$

Analytical Methods

The analytical approach finds an analytical expression which fits the observed data. This method is appropriate, especially when the observations are too sparse. Due to their strongly skewed nature, the loss distributions are usually heavy tailed. The log-normal, Pareto, Burr, Gamma, Exponential and Weibull distributions or *power-law distributions* are often proposed in the literature to depict loss continuous distributions of certain catastrophic natural events, Barton and Nishenko (1994).

In the domain $\mathbb{R}_+$, Burnecki et al. (2000):

- *Log-normal distribution*, with cdf:
$$F(x) = \phi\left(\frac{\ln x - \mu}{\sigma}\right) = \int_0^x \frac{1}{\sqrt{2\pi}\sigma y} e^{-\frac{(\ln y - \mu)^2}{2\sigma^2}} dy, x > 0, \sigma > 0, \mu \in \mathbb{R} \tag{5.5}$$
where $\phi(x)$ is the standard normal distribution function (with mean 0 and variance 1).
- *Pareto distribution*, with cdf:
$$F(x) = 1 - \left(\frac{\lambda}{\lambda + x}\right)^{\alpha}, x > 0, \alpha > 0, \lambda > 0 \tag{5.6}$$
- *Burr distribution*, with cdf:
$$F(x) = 1 - \left(\frac{\lambda}{\lambda + x^{\tau}}\right)^{\alpha}, x > 0, \alpha > 0, \lambda > 0, \tau > 0 \tag{5.7}$$
- *Gamma distribution*, with cdf:
$$F(x) = \int_0^x \frac{1}{\Gamma(\alpha)\beta^{\alpha}} y^{\alpha-1} e^{\frac{-y}{\beta}} dy, x > 0, \alpha > 0, \beta > 0 \tag{5.8}$$
- *Exponential distribution*, with cdf:
$$F(x) = 1 - e^{-\beta x}, x > 0 \tag{5.9}$$
- *Weibull distribution*, with cdf:
$$F(x) = 1 - e^{\beta x^{\tau}}, x > 0, \tau > 0 \tag{5.10}$$

Moment Method

This approach consists of calculating the moments of the distribution. However, using the first four moments (mean, variance, skewness and kurtosis) does not fully characterize the shape of a distribution and the observed data can be poorly fitted. More information about the moment method can be found in Daykin et al. (1994).

Mean excess function

In order to find an accurate loss distribution that fits the loss data one can also compare the shapes of the empirical and the theoretical mean excess function. Given a loss random variable X, the mean excess function (MEF) is the expected payment per insured loss with a fixed amount deductible of x i.e. the mean excess function restricts a random variable X given that it exceeds a certain level x:

$$e(x) = \mathrm{E}(X - x | X > x) = \frac{\int_x^\infty 1 - F(u)du}{1 - F(x)} \tag{5.11}$$

The empirical mean excess function is defined as:

$$\hat{e}_n(x) = \frac{\sum_{x_i > x} x_i}{\#i : x_i > x} - x$$

The next mean excess functions (MEF) are considered to find a proper shape of the analytical distribution to the losses:

- *Log-normal distribution*:

$$e(x) = \frac{e^{\left(\mu + \frac{\sigma^2}{2}\right)} \left\{1 - \Phi\left(\frac{\ln x - \mu - \sigma^2}{\sigma}\right)\right\}}{\left\{1 - \Phi\left(\frac{\ln x - \mu}{\sigma}\right)\right\}} - x$$

- *Pareto distribution*:

$$e(x) = \frac{\lambda + x}{\alpha - 1}, \alpha > 1$$

- *Burr distribution*:

$$e(x) = \frac{\lambda^{\frac{1}{\tau}} \Gamma\left(\alpha - \frac{1}{\tau}\right) \Gamma\left(1 + \frac{1}{\tau}\right)}{\Gamma(\alpha)} \left(\frac{\lambda}{\lambda + x^\tau}\right)^{-\alpha}$$
$$\cdot \left\{1 - B\left(1 + \frac{1}{\tau}, \alpha - \frac{1}{\tau}, \frac{x^\tau}{\lambda + x^\tau}\right)\right\} - x$$

  where

$$\Gamma(\alpha) = \int_0^\infty y^{\alpha - 1} e^{-y} dy$$

  and

$$B(a, b, x) = \frac{\Gamma(a + b)}{\Gamma(a)\Gamma(b)} \int_0^x y^{x-1} (1 - y)^{b-1} dy$$

- *Gamma distribution*:

$$e(x) = \frac{\alpha(1 - F(x, \alpha + 1, \beta))}{\beta(1 - F(x, \alpha, \beta))} - x$$

  where $F(x, \alpha, \beta)$ is the equation (5.8).

- *Exponential distribution*:

$$e(x) = \frac{1}{\beta}$$

- *Weibull distribution*:

$$e(x) = \frac{\Gamma(1+\frac{1}{\tau})}{\beta^{\frac{1}{\tau}}} \left\{ 1 - \Gamma\left(1+\frac{1}{\tau}, \beta x^{\tau}\right) \right\} e^{\beta x^{\tau}} - x$$

Notice that the MEF of the exponential distribution is constant since this distribution function suffers the *loss of memory property*. Whether the information $X > x$ is given or not, the expected value of $X - x$ equals to the expected value of x i.e. as if one started at $x = 0$: $\mathrm{E}(X - x) = \mathrm{E}(x) = \frac{1}{\beta}$. Thus, to find the shape of the MEF one compares the distribution of X with the exponential distribution. When the distribution of X has heavier tails than the exponential distribution the MEF increases and it decreases when the distribution of X shows lighter tails.

Figure 5.7 depicts the empirical mean excess functions for the modeled loss data number 23 of earthquakes in Mexico with and without the outlier of the earthquake in 1985. The left panel shows an increasing pattern for the $\hat{e}_n(x)$, pointing out that the distribution of losses have heavy tails i.e. it indicates that the Log-normal, the Burr or the Pareto distribution are candidates to be the analytical distribution of the loss data. Whereas eliminating the outlier of the earthquake in 1985 from that modeled loss data, the $\hat{e}_n(x)$ shows a decreasing pattern, indicating that Gamma, Weibull or Pareto could model adequately, see right panel of Figure 5.7.

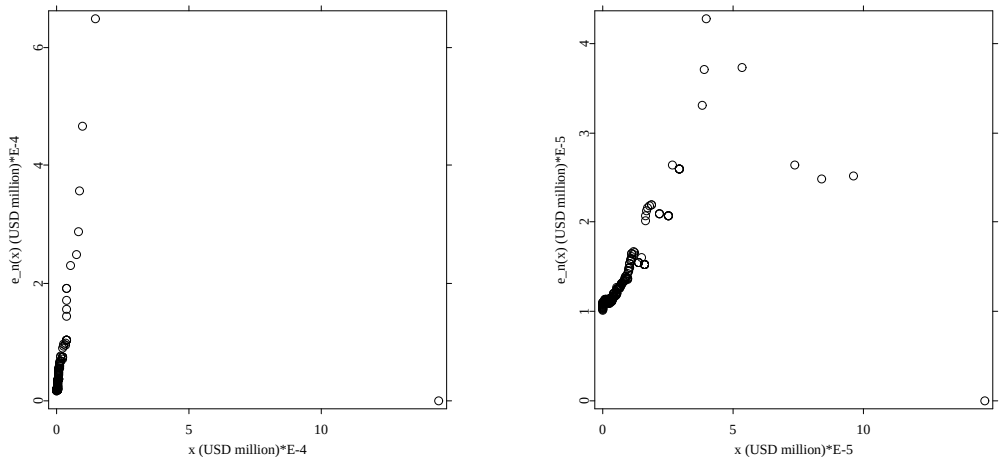

Figure 5.7: The empirical mean excess function $\hat{e}_n(x)$ for the modeled loss data number 23 of earthquakes in Mexico (left panel) and without the outlier of the earthquake in 1985 (right panel)

CMXloss01.xpl

Empirical distribution function tests and parameters estimation

To test whether the fit is adequate, one compares the empirical $F_n(x)$ with the fitted $F(x)$ distribution function. The *edf* statistics measure the difference between these two distributions, D'Agostino and Stephens (1986). To this end the Kolmogorov Sminorv, the Kuiper statistic, the Cramér-von and the Anderson Darling non-parametric tests are applied to check whether values of the fitted distribution function at sample points form a uniform distribution function, Kukla (2000).

- The *Kolmogorov Sminorv statistic* measures the difference between the empirical and the fitted distribution function in the supremum norm:

$$D_n = \sup_{x \in \mathbb{R}} |F_n(x) - F(x)| \tag{5.12}$$

  where the empirical distribution function is defined as, D'Agostino and Stephens (1986):

$$F_n(x) = \frac{1}{n} \sum_{i=1}^{n} I_{\{x_i \leq x\}}$$

- The *Kuiper statistic or V statistic* is defined as:

$$V = D^+ + D^- \tag{5.13}$$

  where $D^+ = \sup_x \{F_n(x) - F(x)\}$ and $D^- = \sup_x \{F(x) - F_n(x)\}$.

- The *Cramér-von Mises statistic* is given by:

$$W^2 = n \int_{\infty}^{\infty} (F_n(x) - F(x))^2 \, dF(x) \tag{5.14}$$

- The Anderson Darling statistic is described as:

$$A^2 = n \int_{-\infty}^{\infty} \frac{(F_n(x) - F(x))^2}{F(x)(1 - F(x))} dF(x) \tag{5.15}$$

The test of the fit procedure consists of the null hypothesis: *the distribution is suitable*, and the alternative: *the distribution is not suitable.*

$$H_0 : F_n(x) = F(x; \theta)$$

$$H_1 : F_n(x) \neq F(x; \theta)$$

where θ is a vector of known parameters. The fit is accepted (no rejection of null hypothesis) when the value of the test is less than the corresponding critical value C_α, given a significance level α. In terms of probability, the null hypothesis will be rejected when the p-value, i.e. $\mathrm{P}(T \geq t)$ is small, where t is the test value for a given sample.

To employ the *edf* tests to the hypothesis that the sample data has a common distribution function $F(x; \theta)$ with θ unknown, it is necessary to estimate the parameters first. When the

parameters are estimated from the data, Ross (2002) overcomes the problem of reducing the critical values for the tests of the specified distribution, by using Monte Carlo simulations. The parameter vector $\hat{\theta}$ is estimated from a sample of size n and the test statistics are calculated according to $F(x, \hat{\theta})$. Then, a sample of size n is created with $F(x, \hat{\theta})$ distributed variables. The new parameter vector $\hat{\theta_1}$ is estimated from this simulated sample and the test statistics are calculated from $F(x, \hat{\theta_1})$. The procedure is repeated until a certain level of precision is reached.

The parameter vector θ can also be estimated, merely finding a $\hat{\theta}^*$ that minimizes a particular *edf* statistic. D'Agostino and Stephens (1986) state that when the fitted distribution $F(x)$ diverge from the true distribution in the tails, the A^2 test is the most potent statistic from the above explained statistics for the estimation scheme. In addition, the A^2 statistic minimization tends to return lower *edf* test statistics values than the maximum likelihood algorithm.

The estimation of parameters via A^2 statistic minimization and the hypothesis testing are computed for the loss models number 8, 22, 23, 24 and 25. The estimated parameters of the best loss model (number 23) and their corresponding *edf* test statistics are shown in Table 5.5. It also shows the corresponding p-values based on 1000 simulated samples in parenthesis. Observe that all the tests reject the fit for all the distributions. However, the loss models with numbers 8, 22 and 25 pass the A^2 statistic for the Burr distribution at the 2%, 1% and 1% level respectively, see Table 5.6, Table 5.7 and Table 5.9. The ranges of the Burr parameters are: $\alpha \in (3.323, 4.008)$, $\lambda \in (16.373, 20.558)$ and $\tau \in (0.886, 0.919)$. The next distribution that passes the A^2 statistic is the Pareto distribution in models number 8 and 22 at the 2% and 0.5% level respectively, see Table 5.6 and Table 5.7. Its parameter ranges are: $\alpha \in (2.199, 2.408)$ and $\lambda \in (11.276, 13.741)$. The other test statistics reject the fits for all distributions.

Distrib.	Log-normal	Pareto	Burr	Exponential	Gamma	Weibull
Parameter	$\mu = 1.456$	$\alpha = 2.199$	$\alpha = 3.354$	$\beta = 0.132$	$\alpha = 0.145$	$\beta = .214$
	$\sigma = 1.677$	$\lambda = 12.53$	$\lambda = 17.33$		$\beta = -0.0$	$\tau = .747$
			$\tau = 0.895$			
D test	0.185	0.142	0.150	0.149	0.299	0.157
	(< 0.005)	(< 0.005)	(< 0.005)	(< 0.005)	(< 0.005)	(< 0.005)
V test	0.308	0.265	0.278	0.245	0.570	0.298
	(< 0.005)	(< 0.005)	(< 0.005)	(< 0.005)	(< 0.005)	(< 0.005)
W^2 test	1.447	0.879	0.987	0.911	6.932	1.16
	(< 0.005)	(< 0.005)	(< 0.005)	(< 0.005)	(< 0.005)	(< 0.005)
A^2 test	10.490	6.131	6.018	10.519	35.428	6.352
	(< 0.005)	(< 0.005)	(< 0.005)	(< 0.005)	(< 0.005)	(< 0.005)

Table 5.5: Parameter estimates by A^2 minimization procedure and test statistics for the modeled loss data number 23 of earthquakes in Mexico. In parenthesis, the related p-values based on 1000 simulations. CMXloss02a.xpl CMXloss02b.xpl

Distrib.	Log-normal	Pareto	Burr	Exponential	Gamma	Weibull
Parameter	$\mu = 1.435$	$\alpha = 2.408$	$\alpha = 4.008$	$\beta = 0.135$	$\alpha = 0.145$	$\beta = 0.212$
	$\sigma = 1.673$	$\lambda = 13.74$	$\lambda = 20.55$		$\beta = .006$	$\tau = .763$
			$\tau = 0.887$			
D test	0.184	0.138	0.147	0.145	0.298	0.154
	(< 0.005)	(< 0.005)	(< 0.005)	(< 0.005)	(< 0.005)	(< 0.005)
V test	0.310	0.261	0.278	0.239	0.569	0.295
	(< 0.005)	(< 0.005)	(< 0.005)	(< 0.005)	(< 0.005)	(< 0.005)
W^2 test	1.347	0.742	0.855	0.741	6.950	0.989
	(< 0.005)	(< 0.005)	(< 0.005)	(< 0.005)	(< 0.005)	(< 0.005)
A^2 test	10.184	5.576	5.431	9.153	5.536	5.674
	(0.02)	(0.02)	(0.02)	(< 0.005)	(< 0.005)	(0.01)

Table 5.6: Parameter estimates by A^2 minimization procedure and test statistics for the modeled loss data number 8 of earthquakes in Mexico. In parenthesis, the related p-values based on 1000 simulations.

Distrib.	Log-normal	Pareto	Burr	Exponential	Gamma	Weibull
Parameter	$\mu = 1.387$	$\alpha = 2.394$	$\alpha = 3.323$	$\beta = 0.143$	$\alpha = 0.143$	$\beta = 0.220$
	$\sigma = 1.644$	$\lambda = 12.92$	$\lambda = 16.67$		$\beta = -0.007$	$\tau = 0.764$
			$\tau = 0.919$			
D test	0.173	0.131	0.137	0.135	0.295	0.145
	(< 0.005)	(< 0.005)	(< 0.005)	(< 0.005)	(< 0.005)	(< 0.005)
V test	0.296	0.248	0.260	0.222	0.569	0.282
	(< 0.005)	(< 0.005)	(< 0.005)	(< 0.005)	(< 0.005)	(< 0.005)
W^2 test	1.358	0.803	0.884	0.790	7.068	1.051
	(< 0.005)	(< 0.005)	(< 0.005)	(< 0.005)	(< 0.005)	(< 0.005)
A^2 test	10.022	5.635	5.563	9.429	36.076	5.963
	(< 0.005)	(0.005)	(0.01)	(< 0.005)	(< 0.005)	(< 0.005)

Table 5.7: Parameter estimates by A^2 minimization procedure and test statistics for the modeled loss data number 22 of earthquakes in Mexico. In parenthesis, the related p-values based on 1000 simulations.

Distrib.	Log-normal	Pareto	Burr	Exponential	Gamma	Weibull
Parameter	$\mu = 1.332$	$\alpha = 2.221$	$\alpha = 3.548$	$\beta = 0.149$	$\alpha = 0.142$	$\beta = .234$
	$\sigma = 1.682$	$\lambda = 11.27$	$\lambda = 16.37$		$\beta = -.007$	$\tau = .748$
			$\tau = 0.886$			
D test	0.175	0.136	0.142	0.139	0.293	0.144
	(< 0.005)	(< 0.005)	(< 0.005)	(< 0.005)	(< 0.005)	(< 0.005)
V test	0.29	0.2411	0.250	0.230	0.548	0.262
	(< 0.005)	(< 0.005)	(< 0.005)	(< 0.005)	(< 0.005)	(< 0.005)
W^2 test	1.356	0.807	0.9053	0.778	6.989	1.041
	(< 0.005)	(< 0.005)	(< 0.005)	(< 0.005)	(< 0.005)	(< 0.005)
A^2 test	9.557	5.552	5.396	9.806	35.781	5.752
	(< 0.005)	(< 0.005)	(< 0.005)	(< 0.005)	(< 0.005)	(< 0.005)

Table 5.8: Parameter estimates by A^2 minimization procedure and test statistics for the modeled loss data number 24 of earthquakes in Mexico. In parenthesis, the related p-values based on 1000 simulations.

Distrib.	Log-normal	Pareto	Burr	Exponential	Gamma	Weibull
Parameter	$\mu = 1.401$	$\alpha = 2.360$	$\alpha = 3.667$	$\beta = 0.1403$	$\alpha = 0.144$	$\beta = .219$
	$\sigma = 1.664$	$\lambda = 12.94$	$\lambda = 18.31$		$\beta = -.007$	$\tau = .760$
			$\tau = .897$			
D test	0.1651	0.1221	0.1294	0.1266	0.2968	0.1349
	(< 0.005)	(< 0.005)	(< 0.005)	(< 0.005)	(< 0.005)	(< 0.005)
V test	0.2802	0.2304	0.245	0.2109	0.5645	0.2632
	(< 0.005)	(< 0.005)	(< 0.005)	(< 0.005)	(< 0.005)	(< 0.005)
W^2 test	1.2964	0.7235	0.8224	0.7204	6.966	0.9663
	(< 0.005)	(< 0.005)	(< 0.005)	(< 0.005)	(< 0.005)	(< 0.005)
A^2 test	9.7782	5.3573	5.236	9.1474	35.6338	5.5523
	(< 0.005)	(< 0.005)	(0.01)	(< 0.005)	(< 0.005)	(< 0.005)

Table 5.9: Parameter estimates by A^2 minimization procedure and test statistics for the modeled loss data number 25 of earthquakes in Mexico. In parenthesis, the related p-values based on 1000 simulations.

Discarding the outlier of the earthquake in 1985, the estimated parameters of the modeled loss number 23 and their hypothesis testing are shown in Table 5.10. It also displays the p-values based on 1000 simulated samples in parenthesis. The exponential distribution with parameter $\beta = 0.1201$ passes all the tests at the 0.8% level, except the A^2 statistic. Likewise, the Pareto distribution passes two tests at very low levels, 0.6% and 1.2%, but with unacceptable fit in the A^2 statistic. All the remaining distributions give worse fits. However, Table 5.11, Table 5.12, Table 5.13 and Table 5.14, display other loss models (number 8,22,24,25) without the outlier of 1985 earthquake, where the Gamma distribution passes all the test statistics and the A^2 statistics at the $0.6\%, 6\%, 5.6\%, 1.8\%$ level respectively.

Distrib.	Log-normal	Pareto	Burr	Exponential	Gamma	Weibull
Parameter	$\mu = 1.493$	$\alpha = 2.632$	$\alpha = 1.8e7$	$\beta = 0.120$	$\alpha = 0.666$	$\beta = 0.194$
	$\sigma = 1.751$	$\lambda = 17.17$	$\lambda = 9.5e7$		$\beta = .070$	$\tau = .770$
			$\tau = 0.770$			
D test	0.116	0.077	0.070	0.081	0.070	0.070
	(< 0.005)	(< 0.005)	(0.001)	(0.084)	(< 0.005)	(0.008)
V test	0.215	0.133	0.126	0.138	0.121	0.126
	(< 0.005)	(0.006)	(< 0.005)	(0.008)	(< 0.005)	(< 0.005)
W^2 test	0.702	0.168	0.166	0.202	0.147	0.166
	(< 0.005)	(0.012)	(< 0.005)	(0.152)	(0.006)	(< 0.005)
A^2 test	6.750	3.022	1.617	4.732	1.284	1.617
	(< 0.005)	(< 0.005)	(< 0.005)	(< 0.005)	(< 0.005)	(< 0.005)

Table 5.10: Parameter estimates by A^2 minimization procedure and test statistics for the modeled loss data number 23 of earthquakes in Mexico, without the outlier of the 1985 earthquake. In parenthesis, the related p-values based on 1000 simulations.

Distrib.	Log-normal	Pareto	Burr	Exponential	Gamma	Weibull
Parameter	$\mu = 1.462$	$\alpha = 2.135$	$\alpha = 3.8e6$	$\beta = 0.119$	$\alpha = 0.634$	$\beta = .206$
	$\sigma = 1.820$	$\lambda = 13.11$	$\lambda = 1.8e7$		$\beta = .005$	$\tau = 0.742$
			$\tau = 0.742$			
D test	0.114	0.074	0.066	0.094	0.065	0.066
	(< 0.005)	(0.006)	(0.01)	(0.01)	(0.026)	(0.018)
V test	0.2257	0.1266	0.122	0.152	0.119	0.122
	(< 0.005)	(0.012)	(< 0.005)	(< 0.005)	(< 0.005)	(< 0.005)
W^2 test	0.687	0.212	0.150	0.299	0.116	0.150
	(< 0.005)	(< 0.005)	(< 0.005)	(0.03)	(0.05)	(0.01)
A^2 test	6.485	3.452	1.487	5.644	1.063	1.487
	(< 0.005)	(< 0.005)	(< 0.005)	(< 0.005)	(0.006)	(< 0.005)

Table 5.11: Parameter estimates by A^2 minimization procedure and test statistics for the modeled loss data number 8 of earthquakes in Mexico, without the outlier of the 1985 earthquake. In parenthesis, the related p-values based on 1000 simulations.

The next distribution that passes all the tests is the Weibull distribution for the loss models number 22 and 24, which pass the A^2 statistics at 1% and 1.2% level, see Table 5.12 and Table 5.13. The Pareto distribution also passes other *edf* tests, but only for the model 22 (Table 5.12) the Anderson-Darling statistic accepts the fit at 3% level. The ranges of the Gamma parameters are: $\alpha \in (0.593, 0.666)$ and $\beta \in (0.059, 0.070)$, the range parameters for the Weibull distribution are: $\beta \in (0.194, 0.209)$ and $\tau \in (0.706, 0.770)$ and the Pareto distribution parameters are in the ranges $\alpha \in (1.585, 2.632)$ and $\lambda \in (8.825, 13.119)$.

Distrib.	Log-normal	Pareto	Burr	Exponential	Gamma	Weibull
Parameter	$\mu = 1.453$	$\alpha = 2.010$	$\alpha = 1.7e7$	$\beta = 0.120$	$\alpha = 0.629$	$\beta = 0.209$
	$\sigma = 1.807$	$\lambda = 11.19$	$\lambda = 8.5e7$		$\beta = 0.065$	$\tau = 0.738$
			$\tau = 0.739$			
D test	0.104	0.071	0.055	0.090	0.052	0.055
	(< 0.005)	(0.03)	(0.4)	(0.05)	(1.12)	(0.52)
V test	0.204	0.120	0.104	0.156	0.099	0.104
	(< 0.005)	(0.05)	(0.2)	(< 0.005)	(0.52)	(0.27)
W^2 test	0.616	0.185	0.125	0.313	0.098	0.125
	(< 0.005)	(0.02)	(0.06)	(0.1)	(0.42)	(0.1)
A^2 test	6.008	3.139	1.267	5.694	0.9047	1.267
	(< 0.005)	(0.03)	(0.01)	(< 0.005)	(0.06)	(0.01)

Table 5.12: Parameter estimates by A^2 minimization procedure and test statistics for the modeled loss data number 22 of earthquakes in Mexico, without the outlier of the 1985 earthquake. In parenthesis, the related p-values based on 1000 simulations.

Distrib.	Log-normal	Pareto	Burr	Exponential	Gamma	Weibull
Parameter	$\mu = 1.441$	$\alpha = 1.585$	$\alpha = 5.6e5$	$\beta = 0.117$	$\alpha = 0.593$	$\beta = 0.220$
	$\sigma = 1.882$	$\lambda = 8.825$	$\lambda = 2.5e6$		$\beta = .059$	$\tau = .706$
			$\tau = 0.769$			
D test	0.114	0.077	0.063	0.104	0.060	0.063
	(< 0.005)	(0.008)	(0.016)	(< 0.005)	(0.032)	(0.04)
V test	0.223	0.134	0.117	0.185	0.104	0.117
	(< 0.005)	(< 0.005)	(< 0.005)	(< 0.005)	(0.05)	(0.024)
W^2 test	0.598	0.250	0.119	0.479	0.08	0.119
	(< 0.005)	(< 0.005)	(0.016)	(< 0.005)	(0.188)	(0.056)
A^2 test	5.694	3.662	1.176	7.193	0.736	1.176
	(< 0.005)	(< 0.005)	(< 0.005)	(< 0.005)	(0.056)	(0.012)

Table 5.13: Parameter estimates by A^2 minimization procedure and test statistics for the modeled loss data number 24 of earthquakes in Mexico, without the outlier of the 1985 earthquake. In parenthesis, the related p-values based on 1000 simulations.

Distrib.	Log-normal	Pareto	Burr	Exponential	Gamma	Weibull
Parameter	$\mu = 1.474$	$\alpha = 2.054$	$\alpha = 1.7e7$	$\beta = 0.118$	$\alpha = 0.631$	$\beta = 0.205$
	$\sigma = 1.808$	$\lambda = 12.59$	$\lambda = 8.3e7$		$\beta = .064$	$\tau = .740$
			$\tau = 0.741$			
D test	0.106	0.072	0.057	0.093	0.056	0.057
	(< 0.005)	(< 0.005)	(0.060)	(0.024)	(0.108)	(0.102)
V test	0.209	0.120	0.106	0.157	0.103	0.106
	(< 0.005)	(0.016)	(0.022)	(< 0.005)	(0.080)	(0.068)
W^2 test	0.629	0.185	0.127	0.305	0.100	0.127
	(< 0.005)	(< 0.005)	(0.008)	(0.034)	(0.080)	(0.024)
A^2 test	6.153	3.192	1.309	5.628	0.927	1.309
	(< 0.005)	(< 0.005)	(< 0.005)	(< 0.005)	(0.018)	(< 0.005)

Table 5.14: Parameter estimates by A^2 minimization procedure and test statistics for the modeled loss data number 25 of earthquakes in Mexico, without the outlier of the 1985 earthquake. In parenthesis, the related p-values based on 1000 simulations.

Consequently, since the Burr and Pareto distribution pass the A^2 statistic with the highest p-values, they are suggested as the analytical distributions for the loss data of earthquakes. Following the same criterion for the case when the outlier of the earthquake in 1985 is neglected, the Gamma, Weibull and Pareto distributions are recommended to model analytically the loss data. Several candidates were taken into account as the choice of the loss distribution is very important because it will influence the CAT bond price.

Limited Expected Value function

For a fixed amount deducible of x, the limited expected value function characterizes the expected amount per loss retained by the insured in a policy, Cizek et al. (2005):

$$L(x) = \mathrm{E}\left\{\min(X, x)\right\} = \int_0^x y dF(y) + x\left\{1 - F(x)\right\}, x > 0 \tag{5.16}$$

where X is the loss amount random variable, with cdf $F(x)$. The empirical estimate is given by:

$$\hat{L}_n(x) = \frac{1}{n}\left(\sum_{x_j<x} x, + \sum_{x_j>x} x\right)$$

The limited expected value function has the following properties:

1. L is a concave, continuous and increasing function.
2. When $x \to \infty$, $L(x) - \mathrm{E}(x)$.
3. Let $L'(x)$ be the derivative of the function L evaluated at point x, and the cdf F operate on the probability scale (0,1), then $F(x) = 1 - L'(x)$.

Besides curve-fitting purposes, the limited expected function is very useful because it emphasizes how different parts of the loss distribution function contribute to the price of the insurance. The next limited expected functions are taken into account to find an adequate distribution to the loss data of earthquakes in Mexico:

- *Log-normal distribution*:

$$L(x) = e^{\left(\mu+\frac{\sigma^2}{2}\right)}\Phi\left(\frac{\ln x-\mu-\sigma^2}{\sigma}\right)+x\left\{1-\Phi\left(\frac{\ln x-\mu}{\sigma}\right)\right\}$$

- *Pareto distribution*:

$$L(x) = \frac{\lambda-\lambda^{\alpha}(\lambda+x)^{1-\alpha}}{\alpha-1}$$

- *Burr distribution*:

$$L(x) = \frac{\lambda^{\frac{1}{\tau}}\Gamma\left(\alpha-\frac{1}{\tau}\right)\Gamma\left(1+\frac{1}{\tau}\right)}{\Gamma(\alpha)}B\left(1+\frac{1}{\tau};\alpha-\frac{1}{\tau};\frac{x^{\tau}}{\lambda+x^{\tau}}\right)+x\left(\frac{\lambda}{\lambda+x^{\tau}}\right)^{\alpha}$$

- *Gamma distribution*:

$$L(x) = \frac{\alpha}{\beta}F(x,\alpha+1,\beta)+x\left\{1-F\left(x,\alpha,\beta\right)\right\}$$

  where $F(x,\alpha,\beta)$ is the equation (5.8).

- *Exponential distribution*:

$$L(x) = \frac{1}{\beta}\left\{1-e^{-\beta x}\right\}$$

- *Weibull distribution*:

$$L(x) = \frac{\Gamma\left(1+\frac{1}{\tau}\right)}{\beta^{\frac{1}{\tau}}}\Gamma\left(1+\frac{1}{\tau},\beta x^{\alpha}\right)+xe^{-\beta x^{\alpha}}$$

A suitable distribution that fits the loss data of earthquakes can be found comparing the limited expected function of the observed data $\hat{L}_n$ with the limited expected function of the analytical distribution L. The closer they are, the better they fit and the closer the mean values of both distributions are. Figure 5.8 presents the empirical and analytical limited expected value functions for the analyzed data set with modeled loss number 23 (left panel) with and without the earthquake in 1985 (right panel). The graphs give explanation for the choice of the Burr, Pareto, Gamma and Weibull distributions. Hence, the prices of the CAT bonds will be based on these distributions.

5.3 Earthquake frequency

Let $(\Omega,\mathcal{F},\mathcal{F}_t,P)$ be a probability space and $\mathcal{F}_t\subset\mathcal{F}$ an increasing filtration, with time $t\in[0,T]$. The number of earthquakes in the interval (0,t] is described by the point process $N_{t\geq 0}$. This process is generated using the times when the ith earthquake occurs T_i, or using the time period

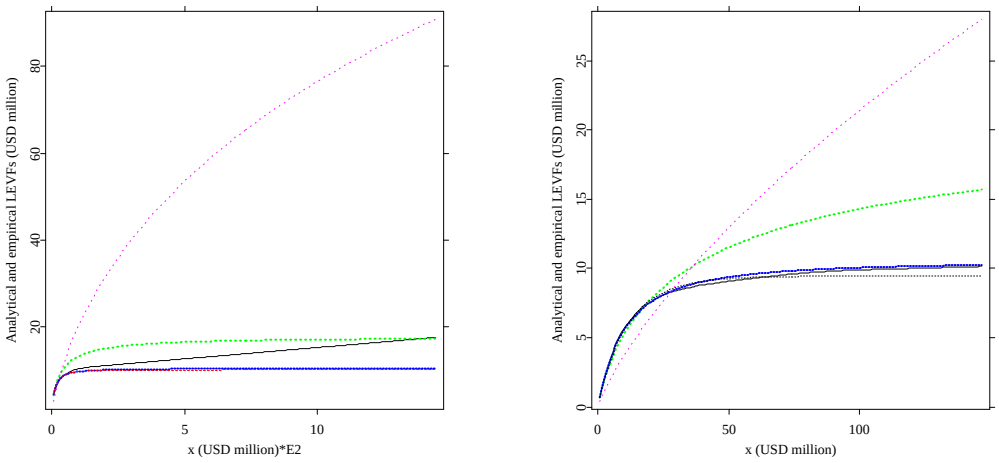

Figure 5.8: The empirical $\hat{l}_n(x)$ (black solid line) and analytical limited expected value function $l(x)$ for the log-normal (green dashed line), Pareto (blue dashed line), Burr (red dashed line), Weibull (magenta dashed line) and Gamma (black dashed line) distributions for the modeled loss data number 23 of earthquakes in Mexico (left panel) and without the outlier of the 1985 earthquake (right panel)

CMXloss02e.xpl CMXloss02f.xpl

between earthquakes $W_i = T_i - T_{i-1}$, defined as waiting times. The earthquake process N_t in terms of W_t's is set by equation (4.1):

$$N_t = \sum_{n=1}^{\infty} I_{(T_n<t)}$$

It is important to remark that earthquakes face a limited size of the sample of historical events (a tail problem), since the recurrence time (waiting time between events) of large earthquakes in a given area can be of several years. Experts in geography believe that certain faults build up stress at a constant rate and will liberate it periodically when it reaches certain levels. In other words, this time dependent hypothesis assumes that the probability of an event ocurring at a given location increases as the time period. Further, recurrence intervals increase with the magnitude of the earthquake and, for large earthquakes, can be in hundreds or thousands years, Anderson, et al. (1998). The evidence and acceptance on the validity and application of time dependent modelling is growing. See for example, the Open File Report (1988).

Many catastrophe modelling firms, such as Risk Management Solution (RMS), Applied Insurance Research (AIR), EQECAT, Risk Engineering, and others, overcome the tail problem combining the use of historical data with certain parametric assumptions about the probability distribution of the characteristics of the earthquakes. However, the accurate modelling of earthquakes is still difficult.

In this thesis, the arrival process of earthquakes in Mexico is modelled with a homogeneous

Poisson process (HPP), Non- homogeneous Poisson process (NHPP), Doubly Stochastic Poisson Process and the renewal process. For generation of the arrival time process, see Ross (2002), Rolski et al. (1999) and Grandell (1999).

5.3.1 Homogeneous Poisson Process (HPP)

An homogeneous Poisson process (HPP) is a continuous-time stochastic process $N_t : t \geq 0$ with intensity $\lambda > 0$ if, Cizek et al. (2005):

- N_t is a point process governed by the Poisson law.
- The waiting times $W_i = T_i - Ti - 1$ are independent identically and exponentially distributed with intensity λ.

The expected value of a HPP is defined as:

$$\mathrm{E}(N_t) = \lambda t \tag{5.17}$$

Figure 5.9 shows the trajectories of the HPP in one thousand years for the intensities: $\lambda_1 = 0.0215$ (blue line), $\lambda_2 = 0.0237$ (green line) and $\lambda_3 = 0.0289$ (red line). Clearly the jumps of the trajectory are more often when λ is higher.

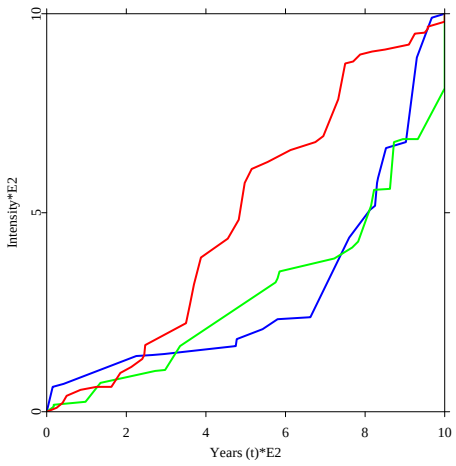

Figure 5.9: Trajectories of a HPP in 1000 years for the intensities $\lambda_1 = 0.0215$ (blue line), $\lambda_2 = 0.0237$ (green line) and $\lambda_3 = 0.0289$ (red line)

CMXrisk01.xpl

5.3.2 Non-homogeneous Poisson Process (NHPP)

The non-Homogenous Poisson (NHPP) is a continuous-time stochastic process $N_t : t >= 0$ with a deterministic intensity function λ_t, if:

- N_t is a point process governed by the Poisson law.
- The waiting times $W_i = T_i - T_{i-1}$ are independent identically and exponentially distributed with intensity λ.
- The increment $N_t - N_s$, with $0 < s < t$, is Poisson distributed with intensity $\tilde{\lambda} = \int_s^t \lambda_u du$. The distribution function of the waiting times is given by:

$$F_s = \mathrm{P}(W_s \leq t) = 1 - \mathrm{P}(W_t \geq t) = 1 - \mathrm{P}(N_{s+t} - N_t = 0)$$

$$= 1 - e^{\left\{-\int_s^{s+t} \lambda_u du\right\}} = 1 - e^{\left\{-\int_0^t \lambda_{s+v} dv\right\}}$$

The expected value of a NHPP is given by:

$$\mathrm{E}(N_t) = \int_0^t \lambda_s ds \tag{5.18}$$

Note that the HPP is the special case of an NHPP when λ_t is a constant. The NHPP is usually used to describe the dependence of the arrival process of natural events on the time of the year, i.e. the seasonality effect of the natural events.

5.3.3 Doubly Stochastic Poisson Process

The doubly stochastic Poisson Process is also called Cox Process or Two-step randomization process. It is defined as a Poisson process N_t conditional on an intensity process Λ_t, which itself is a stochastic process. When Λ_t is deterministic, then N_t is a NHPP, Cizek et al. (2005).

The expected value of a Doubly Stochastic Poisson Process is given by:

$$\mathrm{E}(N_t) = \int_0^t \Lambda_s ds \tag{5.19}$$

5.3.4 Renewal Process

It assumes that the sequence of waiting times $\{W_1, W_2...\}$ of the earthquake arrival point process N_t are positive and independent and identically distributed (i.i.d) variables, i.e. they are generated by a renewal process. In particular, the HPP is the case when the arrival times of a renewal process are exponentially distributed. For more details, see Burnecki et al. (2004).

5.3.5 Simulating the earthquake arrival process

As suggested in the previous section, it is necessary to look for a suitable distribution that models the arrival process of earthquakes. One can achieve that examining the empirical mean excess function $\hat{e}_n(t)$ for the waiting times of the earthquake data, see left panel of Figure 5.10. The empirical mean excess function plot shows an increasing starting and a decreasing ending behaviour, implying that the exponential, Gamma, Pareto and Log-normal distribution could be possible candidates to fit the arrival process of earthquakes. However, for a large t, the tails of the analytical distributions fitted to the earthquake data are different from the one of the empirical distribution. The analytical mean excess functions $e(t)$ increase with time. See right panel of Figure 5.10.

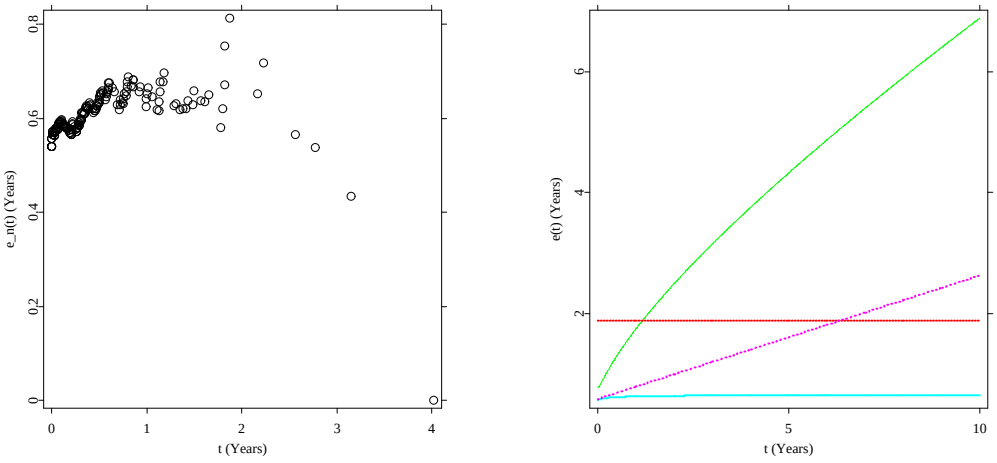

Figure 5.10: The empirical mean excess function $\hat{e}_n(t)$ for the earthquakes data (left panel) and the mean excess function $e(t)$ for the log-normal (green solid line), exponential (red dotted line), Pareto (magenta dashed line) and Gamma (cyan solid line) distributions for the earthquakes data in Mexico (right panel)

CMXrisk02.xpl

To model the claim arrival process of earthquakes by a renewal process, one estimates the parameters of the candidate analytical distributions via the A^2 minimization procedure and tests the Goodness of fit. The estimated parameters and their corresponding p-values based on 1000 simulations are illustrated in Table 5.15. Observe that the exponential, Pareto and Gamma distributions pass all the tests at a very high level. The Gamma distribution passes the A^2 test with the highest level (88%).

Distrib.	Log-normal	Exponential	Pareto	Gamma
Parameter	$\mu = -1.158$	$\beta = 1.880$	$\alpha = 5.875$	$\alpha = 0.858$
	$\sigma = 1.345$		$\lambda = 2.806$	$\beta = 1.546$
D test	0.072	0.045	0.035	0.037
	(0.005)	(0.538)	(0.752)	(0.626)
V test	0.132	0.078	0.067	0.064
	(< 0.005)	(0.619)	(0.719)	(0.739)
W^2 test	0.212	0.062	0.031	0.030
	(< 0.005)	(0.451)	(0.742)	(0.730)
A^2 test	2.227	0.653	0.287	0.190
	(< 0.005)	(0.253)	(0.631)	(0.880)

Table 5.15: Parameter estimates by A^2 minimization procedure and test statistics for the earthquake data. In parenthesis, the related p-values based on 1000 simulations. CMXrisk02a.xpl CMXrisk02b.xpl

If the claim arrival process of earthquakes is modelled with an HPP, the estimation of the annual intensity is obtained by taking the mean of the daily number of earthquakes times 360, i.e. $\lambda = (0.005140)(360)$ equal to 1.8504 earthquakes higher than 6.5 Mw per year. Comparing this annual intensity with the annual intensity of the renewal process modelled with an exponential distribution equal to 1.88 indicates that the earthquakes arrival process can be correctly model with the HPP.

In addition, the arrival process of earthquakes is also modelled with a NHPP. To this end, the mean value function is estimated to the accumulated number of earthquakes N_t or the parameters are estimated by fitting the cumulative intensity function, see equation (5.18). One can estimate the parameters of the intensity function λ_s using the least squared algorithm, Härdle and Simar (2003):

$$\hat{\beta} = \arg\min_{\beta}\{(x - Y\beta)^T(x - Y\beta)\} = \arg\min_{\beta}\{\epsilon^T\epsilon\} \tag{5.20}$$

where x is the dependent variable that represents the accumulated number of earthquakes N_t, Y is the independent variable that represents the time t and ϵ is the errors vector. The intensity is then the derivative of the fitted regression curve that is given by the integral:

$$\lambda_s = \frac{\partial}{\partial t}\int_0^t \lambda_s ds$$

Different polynomial functions are tested to model the intensity λ_s of the earthquake data, but the constant intensity $\lambda_s^1 = 1.8167$, with a coefficient of determination $r^2 = 0.99$ and standard error $SE = 2.33$ is the best fit. This result shows that the HPP is the best fit to describe the arrival process of earthquakes and confirms the theory of time independence of earthquakes. Earthquakes can strike at any time during the year with same probability, they do not show seasonality as other natural events do. Figure 5.11 depicts the number of earthquakes in Mexico, the accumulated number of earthquakes and the mean value functions E(N_t) of the HPP with intensity rates $\lambda_s = 1.8504$ and $\lambda_s^1 = 1.8167$.

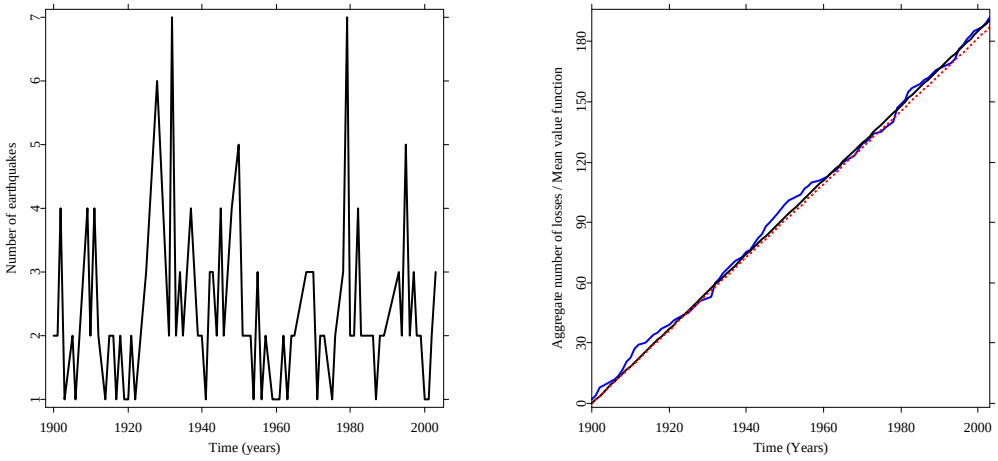

Figure 5.11: Left panel: Number of earthquakes occurred in Mexico during 1900-2003. Right panel: The accumulated number of earthquakes (solid blue line) and mean value functions $\mathrm{E}(N_t)$ of the HPP with intensity $\lambda_s = 1.8504$ (solid black line) and the $\lambda_s^1 = 1.8167$ (dashed red line).

CMXrisk03.xpl

5.4 CAT Bond Pricing Model

In this section the modeled loss is connected to an index CAT bond by means of the compound doubly stochastic Poisson pricing methodology from Baryshnikov et al. (1998) and Burnecki and Kukla (2003), which focuses essentially on the aggregate process L_s and the threshold loss D under continuous trading.

5.4.1 Compound Doubly Stochastic Poisson Pricing Model

The CAT bond is mainly described by, Burnecki and Kukla(2003):

- There is a doubly stochastic Poisson process N_s, Bremaud (1998), describing the flow of a particular catastrophic natural event in a specified region, with an predictable bounded intensity process λ_s, where $s \in [0, T]$. The process λ_s explains the estimates of the natural catastrophe causes.

- The financial losses $\{X_k\}_{k=1}^{\infty}$ caused by these catastrophic events at time t_i are independent and identically distributed random variables (i.i.d) with distribution function $F(x) = \mathrm{P}(X_i < x)$. This is especially valid for the index used as the trigger for the CAT bond.

- The process N_s and X_k are assumed to be independent. Then, the countinuous and

predictable aggregate loss process is:

$$L_t = \sum_{i=1}^{N_t} \tag{5.21}$$

- A continuously compounded discount interest rate r, describing the value at time s of \$1 paid at time $t > s$ by:

$$e^{-R(s,t)} = e^{\int_s^t r(\xi)d\xi}$$

- A threshold time event $\tau = \inf\{t : L_t \geq D\}$, that is the moment when the aggregate loss L_t exceeds the threshold level D. Baryshnikov et al. (1998) defines the threshold time as a point of a doubly stochastic Poisson process $M_t = I_{\{L_t > D\}}$, with a stochastic intensity depending on the index position:

$$\Lambda_s = \lambda_s(1 - F(D - L_s))I_{\{L_s < D\}} \tag{5.22}$$

The choices of the loss distribution and the arrival process of earthquakes are very important because they influence the CAT bond prices. In the previous chapter, for all the loss model datas caused by earthquakes in Mexico, the Burr distribution with parameters ranges $\alpha \in (3.323, 4.008)$, $\lambda \in (16.373, 20.558)$ and $\tau \in (0.886, 0.897)$, passed the A^2 test statistic. The next best fit was the Pareto distribution with parameter ranges $\alpha \in (2.199, 2.408)$ and $\lambda \in (11.276, 13.741)$. Since the outlier of the earthquake in 1985 had a big influence on the quantification of losses, an analytical loss distribution without this observation was also fitted. The Gamma distribution with parameter ranges: $\alpha \in (0.593, 0.666)$ and $\beta \in (0.059, 0.070)$ passed all the goodness of fit tests for most of the loss models. The Weibull distribution with ranges: $\beta \in (0.194, 0.209)$ and $\tau \in (0.706, 0.770)$ was the next best fit, before the Pareto distribution with parameters ranges $\alpha \in (1.585, 2.632)$ and $\lambda \in (8.825, 13.119)$. However, notice that the presence of outliers in the loss data is very characteristic of catastrophic events, the CAT bond essence.

The flow of earthquakes was modelled by an Homogeneous Poisson Process (HPP) with a constant annual intensity $\lambda_s = 1.8504$ and the fitted intensity $\lambda_s^1 = 1.81$ that was obtained with the least squares procedure.

The left panel of Figure 5.12 displays a sample trajectory of the aggregate loss process L_t for one hundred years ($0 \leq t \leq T = 100$ years) simulated with an HPP N_t with intensity $\lambda_s = 1.8504$ and Pareto losses with parameters $\alpha = 2.199$ and $\lambda = 12.533$. It also shows the historical loss trajectory of the loss model data number 23, two sample 5% and 95% quantile lines based on 1000 trajectories of the aggregate loss process and the threshold level $D = \$1600$ million. In addition, it shows the plot of the mean function of the process L_t equal to $\mathrm{E}(L_t) = \left(\frac{\lambda}{\alpha - 1}\right)\lambda t$ only for Pareto losses and a HPP to compare how far the real and the sample loss trajectory are. In this chart, the real aggregate loss process crosses the 5% quantile line, indicating that a heavier tail distribution, like the Burr distribution, would better fit the historical aggregate loss process than the Pareto distribution.

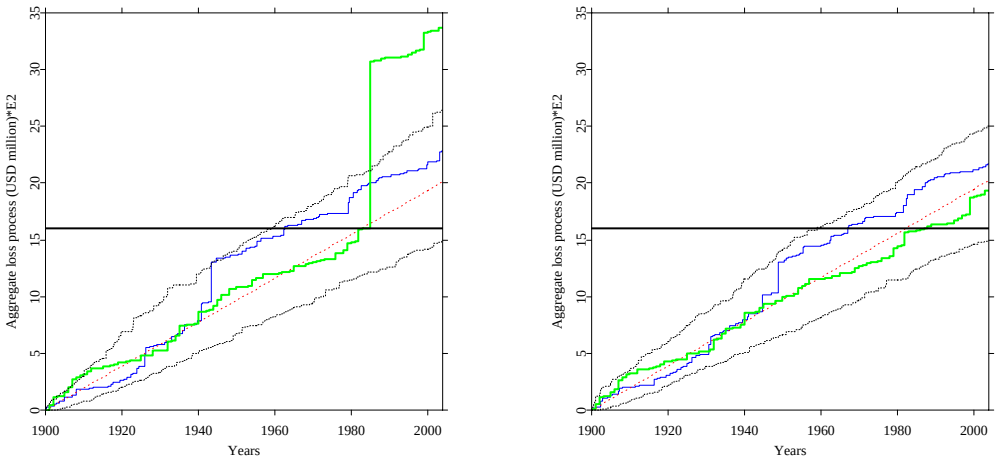

Figure 5.12: Left panel: A sample trajectory of the aggregate loss process L_t (blue solid line), the historical loss trajectory (green line), the analytical mean of the process L_t (dashed red line), 5% and 95% quantile lines (dotted brown lines) and a threshold level $D = 1600$ million for the loss model number 23. Right panel: Same case as the left panel, but the data does not consider the earthquake in 1985.

CMXrisk04e.xpl CMXrisk04f.xpl

In the same way, the right panel of Figure 5.12 presents the case of the loss model data number 23 without the outlier of the earthquake in 1985. It shows one hundred years sample trajectory of the aggregate loss process L_t generated with a HPP N_t with intensity $\lambda_s = 1.8504$ and Pareto losses with parameters $\alpha = 2.6329$ and $\lambda = 17.175$. It also presents the historical loss trajectory without the earthquake in 1985, the mean function of the process L_t, the 5% and 95% quantile lines based on 1000 trajectories of the aggregate loss process and a threshold level $D = \$1600$ million. In this case, the real aggregate loss process falls inside the quantile lines, demonstrating that the Pareto distribution fits adequately.

5.4.2 Zero Coupon CAT bonds

Assume a zero coupon CAT bond that pays a principal amount P at time to maturity T, conditional on the threshold time $\tau > T$. Let P be a predictable process, $P_s = \mathrm{E}(P|\mathcal{F}_s)$ i.e. the payment at maturity is independent from the occurrence and timing of the threshold D. Suppose a process of continuously compounded discount interest rates and assume that in case of occurrence of the trigger event the principal P is fully lost.

The non arbitrage price of the zero coupon CAT bond V_t^1 associated with the threshold D, catastrophic flow process N_s with intensity λ_s, a loss distribution function F and paying the

principal P at maturity is, Burnecky and Kukla (2003):

$$\begin{aligned} V_t^1 &= \mathrm{E}\left[Pe^{-R(t,T)}\left(1-M_T\right)|\mathcal{F}_t\right] \\ &= \mathrm{E}\left[Pe^{-R(t,T)}\left\{1-\int_t^T \lambda_s\left\{1-F(D-L_s)\right\}I_{\{L_s<D\}}d_s\right\}|\mathcal{F}_t\right] \end{aligned} \tag{5.23}$$

To evaluate this zero coupon CAT bond at $t=0$, consider that the continuously compounded discount interest rate $r=5.35\%$ is constant and equal to the London Inter-Bank Offered Rate (LIBOR) in June 2006, FannieMae (2006). Moreover, assume that P=\$160 million, the expiration time $T\in[0.25,3]$ years and a threshold $D\in[\$100,\$135]$ million, corresponding to the 0.7 and 0.8-quantiles of the three yearly accumulated losses of the modeled loss data number 23, i.e. approximately three payoffs are expected to occur in one hundred years (see Table 5.16).

Under these assumptions and after applying 1000 Monte Carlo simulations, in spite of features of instability, the price of the zero coupon CAT bond at $t=0$ is calculated, with respect to the threshold level D and expiration time T, in the Burr and Pareto distribution for the modeled loss data number 23 and the Gamma, Pareto and Weibull distribution for the data without the outlier of the earthquake in 1985. For all the cases the arrival process of earthquakes follows an HPP with constant intensity $\lambda_s=1.8504$.

The plots in Figures 5.13 and 5.14 indicate that the price of the zero coupon CAT bond decreases as the expiration time increases, because the occurrence probability of the trigger event increases. However, the bond price increases as the threshold level increases, since one expects a trigger event with low probability. When $D=\$135$ million and $T=1$ year, the CAT bond price $\$160e^{-0.0535}\approx\$151.658$ is equal to the case when the threshold time $\tau=\inf\{t:L_t>D\}$ is greater than the maturity T with probability one.

Quantile	$3yrsAccL$
10%	18.447
20%	23.329
30%	32.892
40%	44.000
50%	61.691
60%	80.458
70%	**109.11**
80%	**119.86**
90%	142.72
100%	1577.6

Table 5.16: Quantiles of 3 years accumulated loss for the modeled loss data number 23 ($3yrsAccL$) CMXthreshold.xpl

Altough the prices are pretty similar, observe that the loss distribution function influences the price of the CAT bond. For the modeled loss data 23, the Pareto distribution gives higher

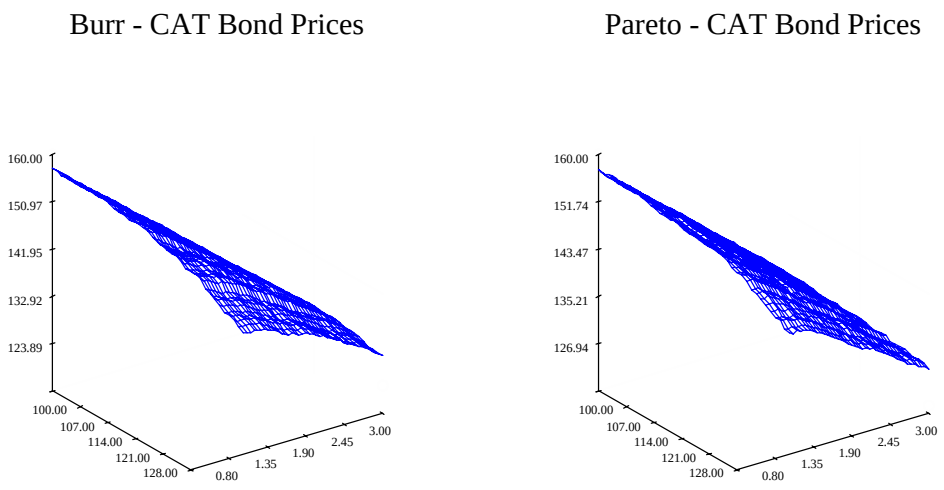

Figure 5.13: The zero coupon CAT bond price (vertical axis) with respect to the threshold level (horizontal left axis) and expiration time (horizontal right axis) in the Burr-HPP (left side) and Pareto-HPP (right side) cases for the modeled loss data number 23.

CMX05e.xpl

prices than the Burr distribution, the difference varies from -2.64% to 0.61% of the principal $P = 160$, see Table 5.17. The zero coupon bond price with respect to expiration time T and threshold level D are more volatile in the case of the Burr (Std. deviation = 10.68) than the Pareto distribution (Std. deviation = 10.08).

	Min. (% Principal)	Max. (% Principal)
Diff. ZCB Burr-Pareto	-2.640	0.614
Diff. ZCB Gamma-Pareto	0.195	4.804
Diff. ZCB Pareto-Weibull	-4.173	-0.193
Diff. ZCB Gamma-Weibull	-0.524	1.636

Table 5.17: Minimum and maximum of the differences in the zero coupon CAT bond prices in terms of percentages of the principal, for the Burr-Pareto distributions of the loss model number 23 and the Gamma-Pareto, Pareto-Weibull, Gamma-Weibull distributions of the loss model 23 without the outlier of the earthquake in 1985.

Even though the prices are also pretty similar, for the modeled loss number 23 without the outlier of the earthquake in 1985 the Gamma distribution leads to higher prices than the Weibull and Pareto distributions. For the Gamma and Pareto distribution the difference varies from 0.19% to 4.8% of the principal $P = 160$, for the Pareto and Weibull distribution varies from -4.17% to -0.19% of the principal and for the Gamma and Weibull distribution varies from -0.52% to 1.63% of the principal. The Gamma distribution shows the lowest standard deviation

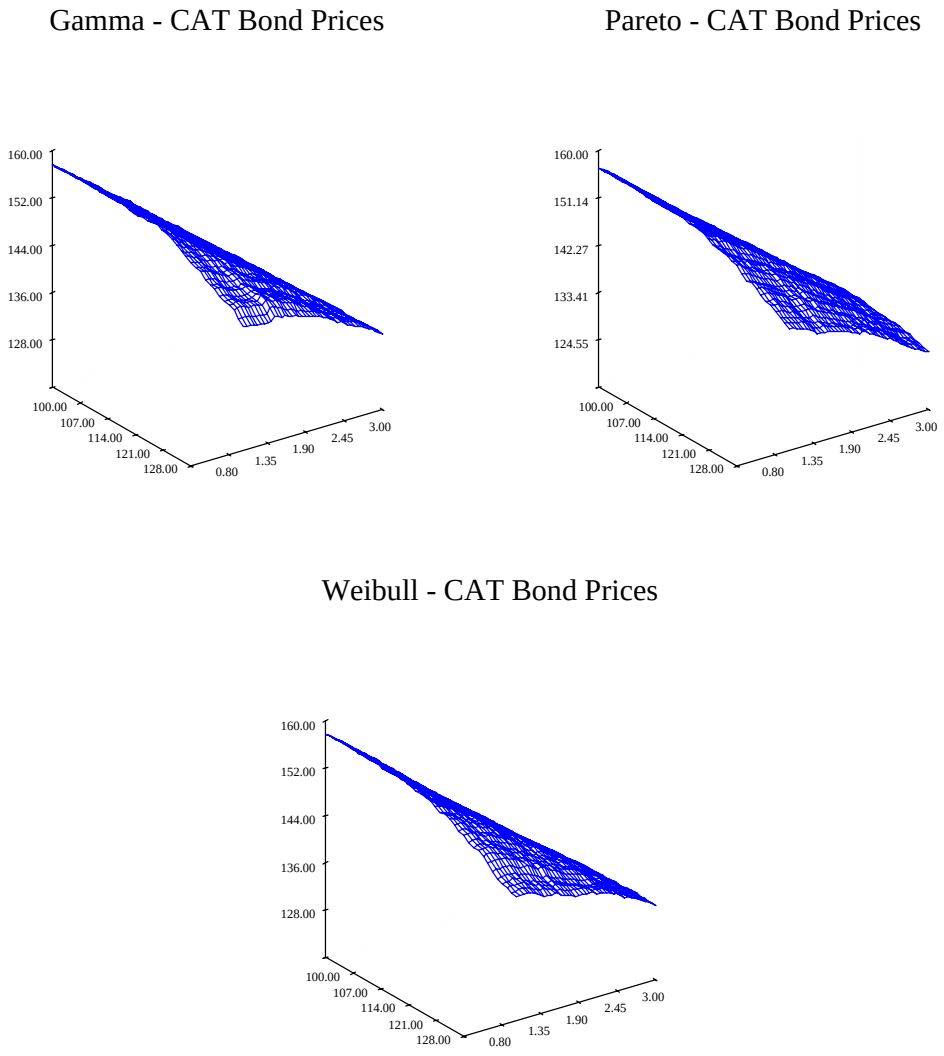

Figure 5.14: The zero coupon CAT bond price (vertical axis) with respect to the threshold level (horizontal left axis) and expiration time (horizontal right axis) in the Gamma-HPP (upper left side), Pareto-HPP (upper right side) and Weibull-HPP (lower side) cases of the modeled loss data number 23, without the earthquake in 1985.

CMX05f.xpl

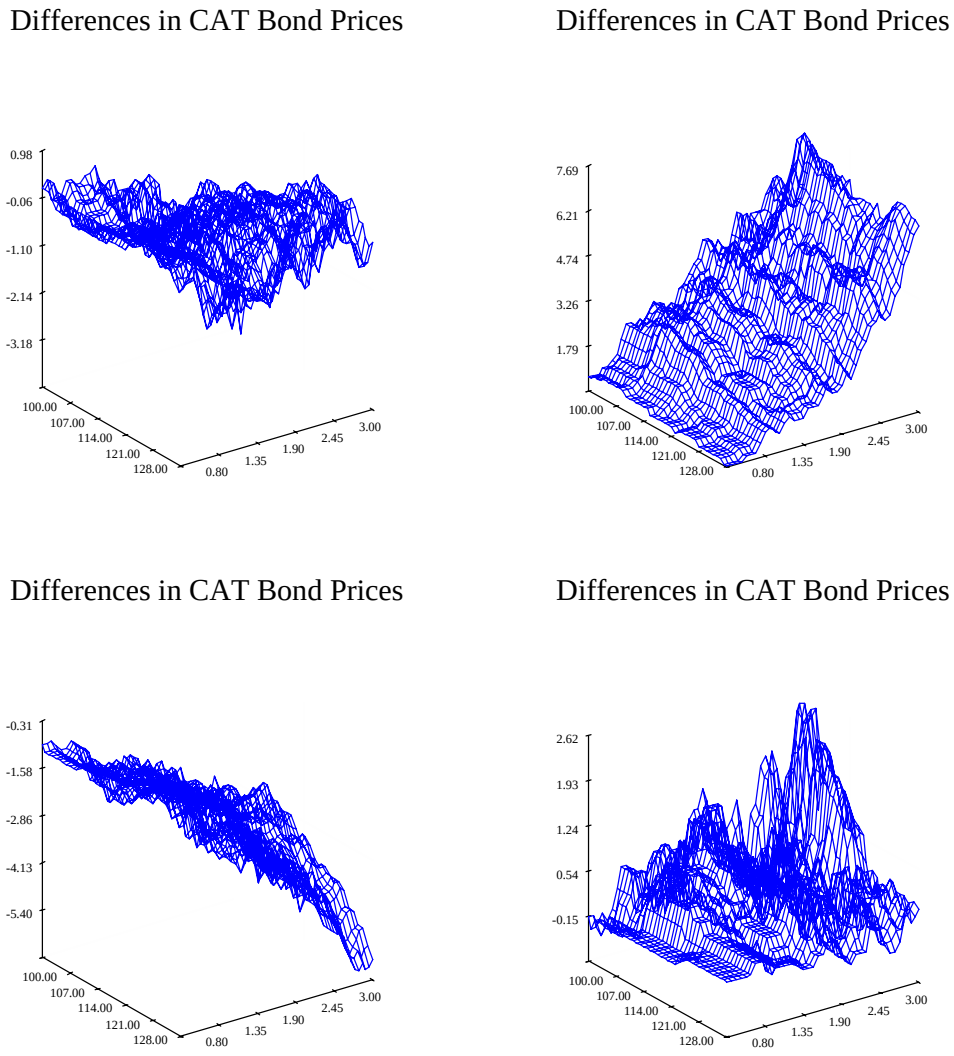

Figure 5.15: The difference in zero CAT bond price (vertical axis) between the Burr and Pareto (upper left side), the Gamma and Pareto (upper right side), the Pareto and Weibull (lower left side) and the Gamma and Weibull (lower right side) distributions under an HPP, with respect to the threshold level (horizontal left axis) and expiration time (horizontal right axis).

CMX06e.xpl CMX06f.xpl

(equal to 8.83) of the zero coupon bond price with respect to expiration time T and threshold level D, comparing to the standard deviations of the Pareto distribution (equal to 10.44) and Weibull distribution (equal to 9.05). The difference in the zero coupon CAT bond price for the different distributions with respect to expiration time T and threshold level D are plotted in Figure 5.15

5.4.3 Coupon CAT bonds

Assume a coupon CAT bond, which pays the principal P at time to maturity T and gives coupon C_t every 3 months until the threshold time τ. Let P be a predictable process $P_s = \mathrm{E}(P|\mathcal{F}_s)$ to be interpreted as the independence of the payment at maturity from the occurrence and timing of the threshold. Suppose a process of continuously compounded discount interest rates and assume that in case of occurrence of the trigger event the principal P is fully lost. This coupons bonds usually pay a fixed spread s over LIBOR. Such spread s reflects the value of the premium paid for the insured event and LIBOR reflects the gain for investing in the bond.

For a given catastrophic flow N_s with intensity rate λ_s, a loss distribution function F and a threshold D, the non arbitrage price of the coupon CAT bond V_t^2 paying P at maturity T and coupons C_s at threshold time τ is given by Burnecky and Kukla (2003):

$$\begin{aligned} V_t^2 &= \mathrm{E}\left[Pe^{-R(t,T)}\left(1-M_T\right)+\int_t^T e^{-R(t,s)}C_s\left(1-M_s\right)ds|\mathcal{F}_t\right] \\ &= \mathrm{E}\left[Pe^{-R(t,T)}+\int_t^T e^{-R(t,s)}\left\{C_s\left(1-\int_t^s \lambda_\xi\left\{1-F(D-L_\xi)\right\}I_{\{L_\xi<D\}}d\xi\right)\right.\right. \\ &\quad \left.\left.-Pe^{-R(s,T)}\lambda_s\left\{1-F(D-L_s)\right\}I_{\{L_s<D\}}\right\}d_s|\mathcal{F}_t\right] \end{aligned} \tag{5.24}$$

Consider that the continuously compounded discount interest rate $r = 5.35\%$, which is constant and equal to the London Inter-Bank Offered Rate (LIBOR) in June 2006, FannieMae (2006). Assume a spread rate s equal to 230 basis points over LIBOR and the principal P equal to \$160 million. The bond has quarterly annual coupons $C_t = \left(\frac{LIBOR+230bp}{4}\right)\$160 = \$3.06$ million. Suposse that the expiration time of the bond $T \in [0.25, 3]$ years and the threshold $D \in [\$100, \$135]$ million that correspond to the 0.7 and 0.8-quantiles of the three yearly accumulated losses of the loss model data number 23 (see Table 5.16). After 1000 Monte Carlo simulations, one obtains the price of the coupon CAT bond at $t = 0$, with respect to the threshold level D and expiration time T, for the Burr and Pareto distribution of the loss model number 23 and for the Gamma, Pareto and Weibull distribution of the modeled loss data number 23 without the outlier of the earthquake in 1985. For all the cases the arrival process of earthquakes follows an HPP with intensity $\lambda_s = 1.8504$.

Figures 5.16 and 5.17 indicate that for all the distributions the price of the coupon CAT bond value increases as the threshold level D increases. But, increasing the expiration time T leads to lower coupon CAT bond prices, because the probability of a trigger event increases and more

coupon payments are expected to be received. Note in Table 5.18 that the coupon CAT prices are higher than the zero coupon CAT prices in Figures 5.13 and 5.14: the maximum absolute value difference between the zero and coupon CAT bond reaches 6.228% of the principal in the Burr distribution and 5.738% in the Pareto distribution for the modeled loss data number 23. For the case without the outlier of the earthquake in 1985 the maximum difference between the zero and coupon CAT bond reaches 7.124% of the principal in the Gamma distribution, 5.25% in the Pareto distribution and 5.29% in the Weibull distribution.

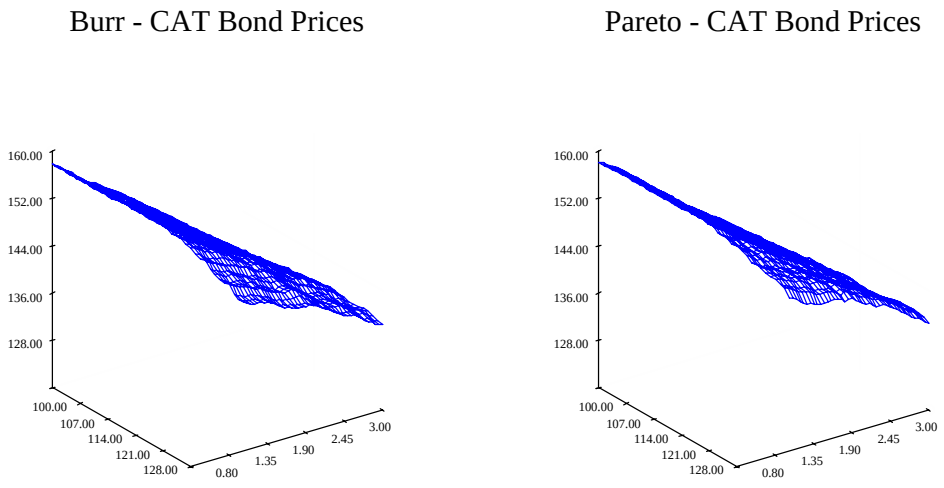

Figure 5.16: The coupon CAT bond price (vertical axis) with respect to the threshold level (horizontal left axis) and expiration time (horizontal right axis) in the Burr-HPP (left side) and Pareto-HPP (right side) cases for the modeled loss data number 23.

CMX07e.xpl

	Min. (% Principal)	Max. (% Principal)
Diff. ZCB-CB Burr	-6.228	-0.178
Diff. ZCB-CB Pareto	-5.738	-0.375
Diff. ZCB-CB Gamma	-7.124	-0.475
Diff. ZCB-CB Pareto (no outlier '85)	-5.250	-0.376
Diff. ZCB-CB Weibull	-5.290	-0.475

Table 5.18: Minimum and maximum of the differences in the zero and coupon CAT bond prices in terms of percentages of the principal, for the Burr and Pareto distributions of the loss model number 23 and the Gamma, Pareto and Weibull distributions of the loss model 23 without the outlier of the earthquake in 1985.

Concerning the loss distribution function for the modeled loss data number 23, the Pareto distribution also leads to higher prices than the Burr distribution. The difference varies from

-1.552% to 0.809% of the principal $P = 160$, see Table 5.19. The Burr distribution also shows a higher standard deviation (equal to 8.31) of the coupon CAT bond price, with respect to expiration time T and threshold level D, than the Pareto distribution (std. deviation = 8.15).

	Min. (% Principal)	Max. (% Principal)
Diff. CB Burr-Pareto	-1.552	0.809
Diff. CB Gamma-Pareto	0.295	6.040
Diff. CB Pareto-Weibull	-3.944	-0.295
Diff. CB Gamma-Weibull	-0.273	3.105

Table 5.19: Minimum and maximum of the differences in the coupon CAT bond prices in terms of percentages of the principal, for the Burr-Pareto distributions of the loss model number 23 and the Gamma-Pareto, Pareto-Weibull, Gamma-Weibull distributions of the loss model 23 without the outlier of the earthquake in 1985.

For the modeled loss number 23 without the outlier of the earthquake in 1985, the Gamma distribution offers higher prices than the Weibull and Pareto distributions. The difference between the Gamma and Pareto distributions varies from 0.295% to 6.04% of the principal $P = 160$, for the Pareto and Weibull distribution varies from -3.944% to -0.295% of the principal and for the Gamma and Weibull distribution varies from -0.273% to 3.105% of the principal. The standard deviation of the coupon bond price with respect to the expiration time T and threshold level D is 6.39 for the Gamma distribution, 8.62 for the Pareto distribution and 7.24 for the Weibull distribution. Figure 5.18 illustrates the difference in the coupon CAT price with respect to expiration time T and threshold level D.

5.4.4 Robustness of the modeled loss CAT bond prices

In order to verify the robustness of the modeled loss with the prices of the zero and coupon CAT bonds one compares the bond prices calculated with different loss models with the bond prices simulated from the pricing algorithm. The bond prices computed from the different loss models are generated with the same seed of the pseudorandom number generator in the 1000 Monte Carlo simulations, while the prices from the pricing algorithm do not use the same seed for their generation.

Define $\hat{P}^*$ as the reference prices or the zero and coupon CAT bond prices of the loss model number 23. Let $\hat{P}_i$ with $i = 1...m$ be the zero or cupon CAT bond price from the ith loss model different to the loss model of the reference prices. The generation of $\hat{P}^*$ and $\hat{P}_i$ is based on the same seed. Furthermore, let $\hat{P}_j$ with $j = 1..n$ be the algorithm CAT bond price obtained in the jth simulation of 1000 trajectories of the zero and coupon CAT bond of the loss model number 23. To check if the type of the model has strong impact on the prices, one computes the mean of *absolute differences* (MAD) i.e. the mean of the differences of the bond prices $\hat{P}_i$ with the reference bond prices $\hat{P}^*$ and the mean of the differences of the algorithm bond prices $\hat{P}_j$ with

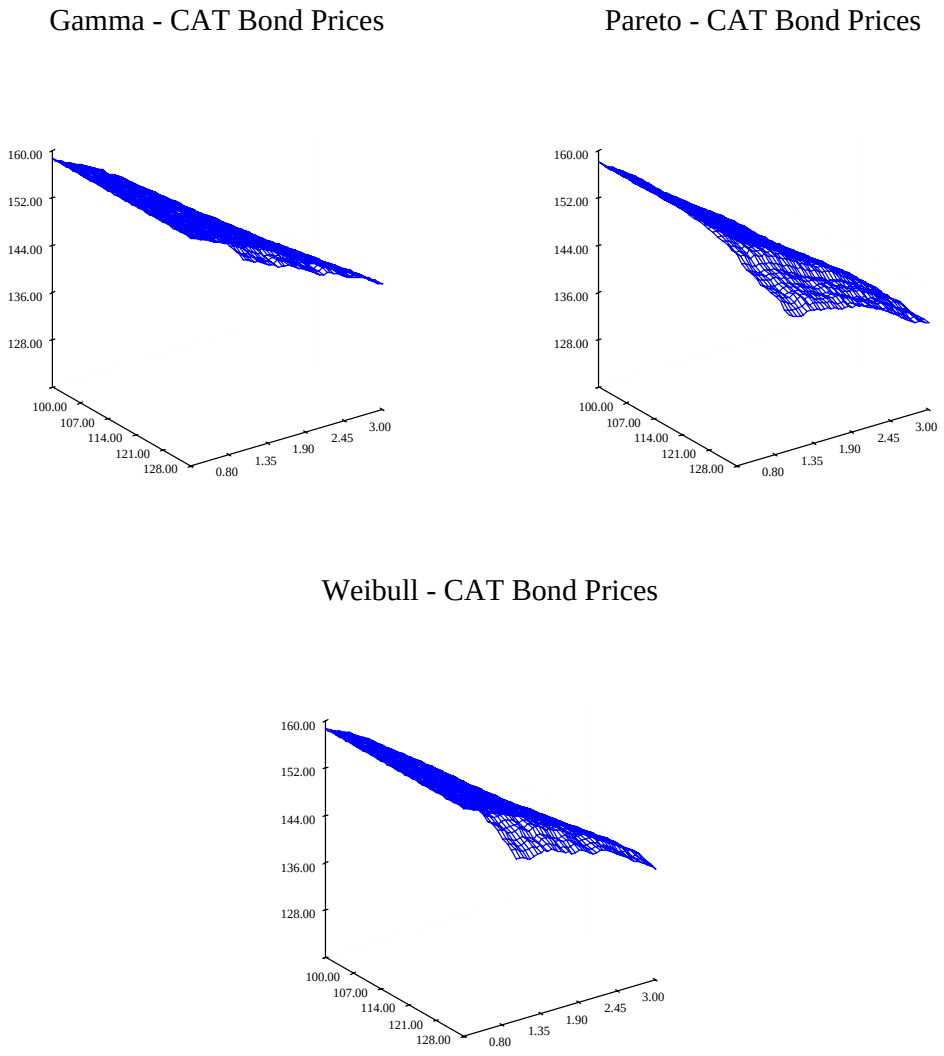

Figure 5.17: The coupon CAT bond price (vertical axis) with respect to the threshold level (horizontal left axis) and expiration time (horizontal right axis) in the Gamma-HPP (upper left side), Pareto-HPP (upper right side) and Weibull-HPP (lower side) cases of the modeled loss data number 23, without the earthquake in 1985.

CMX07f.xpl

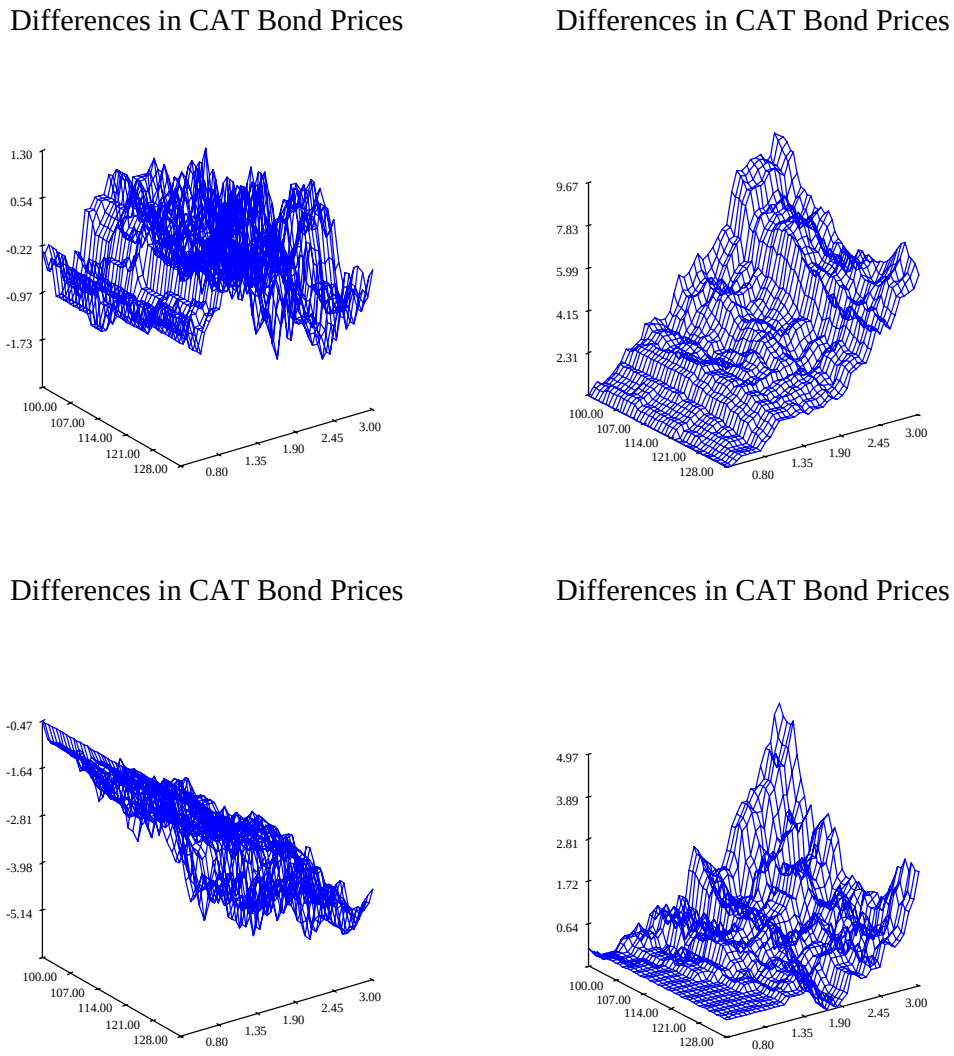

Figure 5.18: Difference in the coupon CAT bond price (vertical axis) between the Burr and Pareto (upper left side), the Gamma and Pareto (upper right side), the Pareto and Weibull (lower left side) and the Gamma and Weibull (lower right side) distributions under an HPP, with respect to the threshold level (horizontal left axis) and expiration time (horizontal right axis)

CMX08e.xpl CMX08f.xpl

the reference bond prices $\hat{P}^*$. If the means of the absolute differences are similar then the type of the model has no influence on the prices of the zero and coupon CAT bond, otherwise it can have:

$$\sum_{i=1}^{m} \frac{\hat{P}_i - \hat{P}^*}{m} \simeq \sum_{j=1}^{n} \frac{\hat{P}_j - \hat{P}^*}{n}, m > 0, n > 0 \tag{5.25}$$

In terms of relative differences, if the means of the absolute values of the relative differences (MAVRD) are similar then the model has no impact on the zero and coupon CAT bond prices:

$$\sum_{i=1}^{m} \frac{1}{m} \left| \frac{\hat{P}_i - \hat{P}^*}{\hat{P}^*} \right| \simeq \sum_{j=1}^{n} \frac{1}{n} \left| \frac{\hat{P}_j - \hat{P}^*}{\hat{P}^*} \right|, m > 0, n > 0 \tag{5.26}$$

Table 5.20 shows the percentages in terms of the reference prices $\hat{P}^*$ (the zero coupon CAT bond prices of the loss model number 23) of the MAD and the MAVRD of the zero coupon CAT bond prices from different loss models (models number 8, 22, 24 and 25) and from the algorithm, with respect to expiration time T and threshold level D. The prices from the algorithm are generated with one hundred simulations of 1000 trajectories of the zero coupon CAT bond prices. Most of the percentages of the MAD of the zero coupon CAT bond prices are not equal to the percentages of the MAD of the algorithm prices, but they are similar (the difference in percentages is less than 1%) meaning that the loss models do not have impact on the zero coupon CAT bond prices. When $T = 2$ years and $D = \$100$ million or $T = 3$ years with $D = \$100, 120, 135$ million, the percentages of the MAVRD from the zero coupon CAT bonds prices differ from the percentages of the MAVRD of the algorithm prices, but in general the percentages of the MAVRD are similar (the difference in percentages is above 0% and less than 2%). This indicates no significant influence of the loss models on the zero coupon CAT bond prices.

T	D	$\hat{P}^*$	(%) MAD_A	(%) MAD_B	(%) $MAVRD_A$	(%) $MAVRD_B$
1	100	148.576	0.283	0.975	0.329	0.265
1	120	149.637	0.203	0.663	0.270	0.228
1	135	149.637	0.619	0.802	0.619	0.183
2	100	133.422	1.577	2.334	1.577	0.566
2	120	137.439	0.823	1.306	0.823	0.375
2	135	138.873	0.884	1.161	0.930	0.358
3	100	114.866	4.666	5.316	4.666	0.859
3	120	123.177	2.409	2.958	2.409	0.640
3	135	125.766	2.468	2.817	2.468	0.520

Table 5.20: Percentages in terms of $\hat{P}^*$ of the MAD and the MAVRD of the zero coupon CAT bond prices from the loss models number 8, 22, 24 and 25 ($MAD_A, MAVRD_A$) and one hundred simulation of 1000 trajectories of the zero coupon CAT bond prices from the algorithm ($MAD_B, MAVRD_B$), with respect to expiration time T and threshold level D. CMXmycheckvar.xpl

In a similar way for the coupon CAT bond prices, Table 5.21 displays the percentages in terms of $\hat{P}^*$ (the coupon CAT bond prices of the modeled loss number 23) of the MAD and the MAVRD of the coupon CAT bond prices from the different loss models (number 8, 22, 24 and 25) and the coupon CAT bond prices from the algorithm, with respect to expiration time T and threshold level D. The algorithm prices are also generated using one hundred simulation of 1000 trajectories of the coupon CAT bond prices. The percentages of the MAD of the coupon CAT bond prices from different loss models are similar to the percentages of the MAD of the algorithm (the difference in percentages is less than 1%). This similarity also holds for the percentages of the MAVRD of the coupon CAT bond prices (the difference in percentages is less than 1.5%). These similarities indicate that the loss models do not have impact on the coupon CAT bond prices.

T	D	$\hat{P}^*$	(%) MAD_A	(%) MAD_B	(%) $MAVRD_A$	(%) $MAVRD_B$
1	100	151.236	0.513	1.152	0.556	0.257
1	120	152.306	0.398	0.853	0.419	0.216
1	135	152.920	0.383	0.601	0.405	0.178
2	100	139.461	0.966	2.131	0.966	0.475
2	120	142.950	0.731	1.585	0.774	0.395
2	135	145.141	0.337	0.827	0.556	0.354
3	100	124.831	2.412	3.421	2.412	0.823
3	120	131.508	1.844	2.590	1.844	0.708
3	135	134.324	2.071	2.474	2.071	0.600

Table 5.21: Percentages in terms of $\hat{P}^*$ of the MAD and the MAVRD of the coupon CAT bond prices from the loss models number 8, 22, 24 and 25 ($MAD_A, MAVRD_A$) and one hundred simulation of 1000 trajectories of the coupon CAT bond prices from the algorithm ($MAD_B, MAVRD_B$), with respect to expiration time T and threshold level D. CMXmycheckvar1.xpl

The previous results reveal no significant impact of the modeled loss on the zero and coupon CAT bond prices. An explanation to this is the quality of the original loss data, where 88% of the data is missing. The expected loss is considerably more important for the CAT bond prices than the entire distribution of losses. This is due to the nonlinear character of the loss function and of the CAT bond price that depend on different variables. An earthquake with two whole numbers magnitude Mw higher than the average strength might do more or less than twice the damage of an earthquake of average strength. The left panel of Figure 5.19 presents the zero coupon CAT bond prices at time to maturity $T = 3$ with respect to the threshold level D. The right panel of Figure 5.19 presents the coupon CAT bond prices at time to maturity $T = 3$ with respect to the threshold level D. Both panels show the CAT bond prices with Burr and Pareto losses for different models. Figure 5.19 shows that the bond prices are more dispersed under different loss models with the same distribution assumption than under different distribution assumptions with the same loss model. This confirms that the expected losses are more important than the distribution of losses.

The relevance of the model loss trigger mechanism is that it considers different variables that influence the underlying risk. Because of quality of the data, the previous empirical study showed that the modeled loss did not have influence on the CAT bond prices. This analysis may be useful in determining whether, for a given expected loss, the risk of earthquake has an impact on how a bond will be priced relative to an *expected level*.

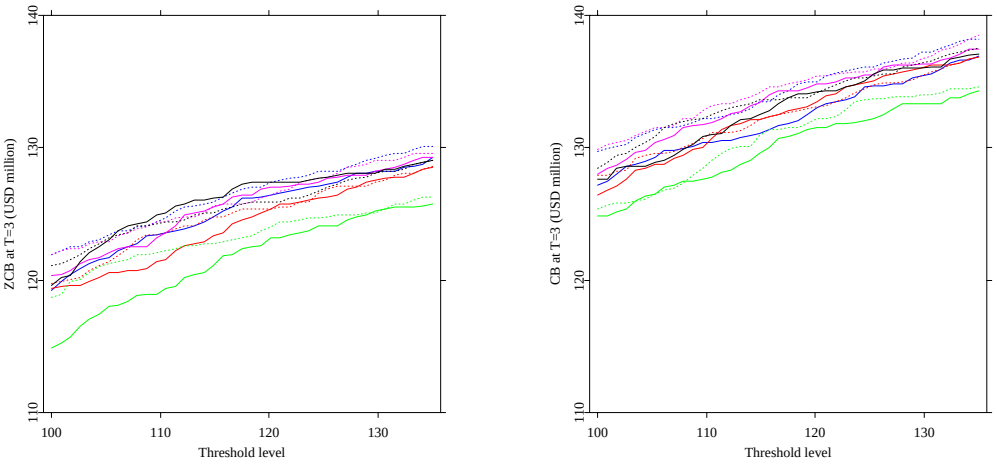

Figure 5.19: The zero coupon (left panel) and coupon (right panel) CAT bond prices at time to maturity $T = 3$ years with respect to the threshold level $D \in [\$100, \$135]$ million. The solid lines are the CAT bond prices under the Burr distribution and the dotted lines are the CAT bond prices under the Pareto distribution. The blue solid and dotted lines correspond to the model 8, the red lines to the model 22, the green lines to the model 23, the magenta to the model 24 and the black lines to the model 25

CMX09.xpl CMX10.xpl

6 Conclusion

Mexico has a high level of seismic activity due to the interaction between the Cocos plate and the North American plate. In the presence of this, the Mexican government has turned to the capital markets to cover costs of potential earthquake catastrophes, issuing a CAT bond that passes the risk on to investors.

This thesis examined the calibration of a real parametric CAT bond that was sponsored by the Mexican government, issued by a special purpose Cayman Islands CAT-MEX Ltd. and structured by Swiss Re AG and Deutsche Bank AG. The calibration of the bond was based on the estimation of the intensity rate that describes the flow process of earthquakes.

Under the assumption of perfect markets, actuarial principles were applied to estimate the intensity rates from the reinsurance and capital markets. The actuarially fair reinsurance price is equal to the expected value of the loss from catastrophes and the fair bond price equals to the expected gains from the bond purchase. In addition the historical intensity rate was estimated using the *intensity model*. This model defines a process B_t to characterize the trigger event process, where the arrival process of earthquakes followed a HPP N_t with intensity $\lambda > 0$ and whose times between earthquakes W_i were exponentially distributed with intensity λ. The process B_t counted only earthquakes that trigger the CAT bond's payoff. However, the dataset contained only three such events, what led to the decomposition of the calibration of the historical intensity rate into the calibration of the intensity of all earthquakes with a magnitude higher than 6.5 Mw and the estimation of the probability of the trigger event.

The intensity rate estimates from the reinsurance λ_1 and capital market λ_2 were approximately equal but they deviated from the historical intensity rate λ_3. The absence of the public and liquid market of earthquake risk in the reinsurance market might explain the small difference between the intensity rates from the reinsurance market and the capital market, just limited information is available. Another reason might be that contracts in the capital market are more expensive than contracts in the reinsurance market when considering other risks, such as the cost of risk capital or the risk of default. The differences between the intensity rates λ_1 and λ_3 or λ_2 and λ_3 could be explained by the presence of just three trigger events in the historical data. The estimation of λ_3 depended on the time period of the historical data. A different period could lead to a lower historical intensity rate. The estimation of λ_3 played an important role when one considered it as a reference intensity rate. It involved different interpretations

about the calibration of the parametric CAT bond.

Assuming that the historical intensity rate would be the adequately correct one, the results demonstrated that the Mexican government paid total premiums equivalent to 0.75 times the real actuarially fair reinsurance price. One reason might be that Swiss Re estimated a probability of an earthquake lower than the one estimated from historical data. Another explanation could be that the value of the premium is not only exponsed to the loss of the insured event, but to other risk such as the credit risk. Under the same assumption of the historical intensity rate, another argument to the low premiums for covering the seismic risk might be the financial strategy of the government, where 35% of the total seismic risk is transferred to the investors. For the government, this strategy that consists of a mix of reinsurance and CAT bond is optimal in the sense that it provides coverage of $450 million for a lower cost than the reinsurance itself.

The decision of the government to issue a parametric CAT bond relies on the fact that it triggers immediately when an earthquake meets the defined physical parameters. There is no threshold for losses, which is more characteristic for CAT bonds issued by insurers and reinsurers. The parametric CAT bond especially helps the government with fast emergency services and rebuilding after a big earthquake.

This thesis also derived the price of an hypothetical CAT bond with a modeled loss trigger mechanism for earthquakes. Besides considering the historical information, a modeled loss trigger mechanism takes other variables into account, like the physical characteristics of an earthquake, that can affect the value of losses. The modeled CAT bond price was based on the compound doubly stochastic Poisson pricing methodology from Baryshnikov et al. (1998) and Burnecki and Kukla (2003), where the trigger event was dependent on the frequency and severity of earthquakes. The threshold event was defined as the time when the accumulated losses L_s exceed the threshold level D. It was modelled with a Poisson process M_t with a stochastic intensity Λ_s depending on the index position. The HPP N_t was the best process to describe the flow of earthquakes.

Another important task was the choice of the analytical distribution that describes adequately the losses, because it influenced the CAT bond prices. The parameter estimations were made via the Anderson-Darling minimisation procedure. The non-parametric tests Kolmogorov Smirnov, Kuiper, Crámer-von Mises and Anderson-Darling were applied to tests the goodness of fit. The Burr, Pareto, Gamma and Weibull distribution were analysed and indicated to be the best fits. For all the distributions and by assuming a HPP, the zero and coupon CAT bond prices were computed. They increased as the threshold level D increased, but decreased as the expiration time T increased. This was mainly because the probability of a trigger event increases and more coupon payments are expected to be received. Because of the quality of the data, the results pointed out that different loss models reveal no impact on the CAT bond prices. Due to the nonlinearity of the loss function and of the CAT bond price, the expected loss was considerably more important for the evaluation of a CAT bond than the entire distribution of losses. This analysis may be useful in determining whether, for a given expected loss, the risk of earthquake

has an impact on how a bond will be priced relative to an *expected level*.

The attractive spread rate offered by both CAT bonds was comparable to the premium paid for the insured event. The spread rate was reflected by the intensity rate of the earthquake process in the parametric trigger mechanism. While for the modeled loss trigger mechanism the spread rate was represented by the intensity rate of the earthquake process and the level of accumulated losses L_s.

This thesis shows that the trigger mechanism matters for the CAT bond pricing, as long as the expected loss or the arrival process of the underlying are adequately estimated. Without doubt, the availability of information and the quality of the data provided by research institutions attempting earthquakes has a direct impact on the accuracy of this risk analysis and for the evaluation of CAT bonds.

The CAT bond market shows a growing trend, but still needs to be adjusted into standard procedures that can be covered with further research. From the point of view of bond holders, the basis risk and moral hazard behaviour of the issuing firm are important factors and should be taken into account when pricing the CAT bond, Lee and Yu (2002). In multi peril CAT bonds, the advance risk model should specify the included risks that are relevant for the pricing of the CAT bond, for example: fire following earthquakes. The CAT bonds pricing should also consider the demand surge (the demand for building materials, repair workers, etc.) that will be reflected later in the inflation. In addition, operational and legal costs must be included in the adjustment of losses when pricing CAT bonds, Anderson et al. (1998).

Bibliography

Aase, K. (1999). An Equilibrium Model of catastrophe Insurance Futures and Spreads, *The Geneva Papers on Risk and Insurance Theory 24*: 69-96.

Anderson, R.,Bendimerad, F., Canabarro, E. and Finkemeier, M. (1998). Fixed Income Research: Analyzing Insurance-Linked Securities, *Quantitative Research*, Goldman Sachs & Co.

Barton, C. and Nishenko, S. (1994). Natural Disasters - Forecasting Economic and Life Losses, *SGS special report*.

Baryshnikov, Y., Mayo, A. and Taylor, D.R. (1999). *Pricing CAT Bonds*, Preprint.

Bremaud, P. (1981). *Point Processes and Queues: Martingale Dynamics*, Springer, New York.

Burnecki, K., Kukla, G. and Weton, R. (2000). *Property insurance loss distributions*, Physica A 287:269-278.

Burnecki, K. and Kukla, G. (2003). Pricing of Zero-Coupon and Coupon CAT Bonds, *Appl. Math (Warsaw) 30(3)*:315-324.

Burnecki, K. and Hrdle, W. and Weron, R. (2004). Simulation of risk processes, in J. Teugels, B. Sundt (eds.), *Encyclopedia of Actuarial Science*,Wiley, Chichester.

Cizek, P., Härdle, W. and Weron, R. (2005). *Statistical Tools for Finance and Insurance*, Springer: 93-104, 289-334.

Clarke, R., Faust, J. and McGhee, C. (2005). *The Growing Appetite for Catastrophic Risk: The Catastrophe Bond Market at Year-End 2004*, Studies Paper. Guy Carpenter & Company, Inc.

Clarke, R., Faust, J. and McGhee, C. (2005). *The Catastrophe Bond Market at Year-End 2005: Ripple Effects from record storms*, Studies Paper. Guy Carpenter & Company, Inc.

Daykin, C.D., Pentikainen, T. and Pesonen, M. (2005). *Practical Risk Theory for Actuaries*, Chapman, London.

D'Agostino and Stephens, M.A. (1986). *Goodness-of-Fit Techniques*, Marcel Dekker, New York.

Dubinsky, W. and Laster, D. (2005). Insurance Link Securities *SIGMA*, Swiss Re publications.

FannieMae. (2006). LIBOR Rate, http://www.fanniemae.com/tools/libor/2006.jhtml

Franke, J., Hrdle, W. and Hafner, C. (2000). *Statistic of Financial Markets*, Springer.

Froot, K. (1999). The Market for Catastrophe Risk: A Clinical Examination, *National Bureau of Economic Research Working Paper No.7286*

Grandell, J. (1999). *Aspects of Risk Theory*, Springer, New York.

Härdle, W. and Simar, L. (2003). *Applied Multivariate Statistical Analysis*, Springer.

Howell, D. and (1998). Treatment of missing data, http://www.uvm.edu/ dhowell/StatPages/More$_{S}tuff/Missing_{D}ata/Missing.html$

IAIS, International Association of Insurance Supervisors. (2003). Non-Life Insurance Securitisation, *Issues Papper*

Kukla, G.(2000). *Insurance Risk Derivatives*, MSc Thesis, Wroclaw Univ. of Technology.

Lane, M.N. (2004). *The Viability and Likely Pricing of CAT Bonds for Developing Countries*, Lane Financial.

Lee, J. and Yu, M. (2002). Pricing Default Risky CAT Bonds with Moral Hazard and Basis Risk, *The Journal of Risk and Insurance, Vol.69, No.1*;25-44.

López, B. (2003). *Valuacin de Bonos Catastrficos para terremotos en Mexico*, Tesis.

McGhee, C. (2004). *Market Update: The Catastrophe Bond Market at Year-End 2003*, Guy Carpenter & Company, Inc.

Mooney, S. (2005). *The World Catastrophe reinsurance market 2005*, Guy Carpenter & Company, Inc.

Rolski, T., Schmidli, H., Schmidt, V., and Teugels, J. L. (1999). *Stochastic Processes for Insurance and Finance*, Wiley, Chichester.

RMS. (2006). Mexico earthquake, www.rms.com/Catastrophe/Models/Mexico.asp

Rosenblueth, E. (2000). *Sismos y sismicidad en Mexico*, Instituto de Ingenieria UNAM.

Ross, S. (2002). *Simulation*. 3rd ed., Academic Press, Boston.

SHCP. (2001). Secretaría de Hacienda y Crédito Público México, *Acuerdo que establece las Reglas de O-peracin del Fondo de Desastres Naturales FONDEN*. Mexico.

SHCP. (2004). Secretaría de Hacienda y Crédito Público México, *Administracin de Riesgos Catastrficos del FONDEN*. Mexico.

SSN Ingenieros: Estrada, J. and Perez, J. and Cruz, J.L and Santiago, J. and Cardenas, A. and Yi , T. and Cardenas, C. and Ortiz, J. and Jiménez, C. (2006). Servicio Sismológico Nacional Instituto de Geosifísica UNAM, *Earthquakes Data Base 1900-2003*.

Sigma. (1996). *Insurance Derivatives and Securitization: New Hedging Perspectives for the US catastrophe Insurance Market?*, Report Number 5, Swiss Re.

Sigma. (1996). *Insurance Derivatives and Securitization: New Hedging Perspectives for the US catastrophe Insurance Market?*, Report Number 5, Swiss Re.

Sigma. (1997). *Too Little Reinsurance of Natural Disasters in Many Markets*, Report Number 7, Swiss Re.

Suárez, G. and Jiménez, Z. (1997). Sismo en la ciudad de Mexico y el terremoto del 19 de septiembre de 1985, *Cuadernos del Instituto de Geofsica* Instituto de Geofsica, UNAM Mxico, D.F.

USGS. (2006). U.S. Geological Survey, http://pubs.usgs.gov/gip/earthq4/severitygip.html

Vaugirard, G. (2002). Valuing catastrophe bonds by Monte Carlo simulations, *Journal Applied Mathematical Finance 10*; 75-90.

Wikipedia, G. (2006). Seismograph, http://en.wikipedia.org/wiki/Wikipedia

Working Group on California Earthquake Probabilities (1998). Probabilities of large earthquakes ocurring in California on the San Andreas Fault, *Open file report*:88-398. U.S. Department of the Interior.